SÃO PAULO STATE UNIVERSITY(UNESP)
SCHOOL OF ENGINEERING
ILHA SOLTEIRA

BRUNO ANTONIO BARBIZAN

NUMERICAL ANALYSIS OF MULTISPLITTER BLADE IMPELLER FOR A CO2 CENTRIFUGAL COMPRESSOR

Ilha Solteira
2024

UNIVERSIDADE ESTADUAL PAULISTA
"JÚLIO DE MESQUITA FILHO"
Campus de Ilha Solteira

BRUNO ANTONIO BARBIZAN

NUMERICAL ANALYSIS OF MULTISPLITTER BLADE IMPELLER FOR A CO2 CENTRIFUGAL COMPRESSOR

Course completation paper presented to the School of Engineering at Ilha Solteira – UNESP as part of requirements for obtaining the title of Mechanical Engineering.

Advisor:
Prof. Dr. Leandro Oliveira Salviano

Ilha Solteira
2024

FICHA CATALOGRÁFICA
Desenvolvido pelo Serviço Técnico de Biblioteca e Documentação

B237n

Barbizan, Bruno Antonio.
Numerical analysis of Multisplitter blade impeller for a CO2 centrifugal compressor / Bruno Antonio Barbizan. -- Ilha Solteira: [s.n.], 2024
50 f. : il.

Trabalho de conclusão de curso (Graduação em Engenharia Mecânica) - Universidade Estadual Paulista (UNESP), Faculdade de Engenharia, Ilha Solteira, 2024

Orientador: Leandro Oliveira Salviano

Inclui bibliografia

1. Centrifugal compressor. 2. Splitters. 3. Sensitivity analysis . 4. CFD.

Elaborado por Raiane da Silva Santos - CRB - 8/9999

UNIVERSIDADE ESTADUAL PAULISTA
"JÚLIO DE MESQUITA FILHO"
Campus de Ilha Solteira

CURSO DE ENGENHARIA MECÂNICA

ATA DA DEFESA - TRABALHO DE GRADUAÇÃO

Ao décimo sétimo dia do mês de Junho de dois mil e vinte e quatro, às quatorze horas e trinta minutos, em reunião pelo Google Meeting (https://meet.google.com/com-zynk-jct), o discente BRUNO ANTONIO BARBIZAN, matriculado sob o RA 162054629, apresentou o Trabalho de Graduação intitulado NUMERICAL ANALYSIS OF MULTISPLITTER BLADE IMPELLER FOR A CO2 CENTRIFUGAL COMPRESSOR, tendo como banca examinadora o PROF. DR. LEANDRO OLIVEIRA SALVIANO (Orientador/Presidente), PROF. DR. ELOY ESTEVES GASPARIN, ENG. RAFAEL SANCHES ELLER. Após exposição e arguição, o discente foi **APROVADO** pela Comissão Examinadora. Encerrada as atividades, lavro a presente Ata.

Comissão Examinadora:

Prof. Dr. Leandro Oliveira Salviano
(Orientador/Presidente) ______________________

Prof. Dr. Elóy Esteves Gasparin ______________________

Eng. Rafael Sanches Eller ______________________

Discente:

Bruno Antonio Barbizan ______________________

Ilha Solteira, 17 de Junho de 2024.

UNIVERSIDADE ESTADUAL PAULISTA "Júlio de Mesquita Filho"
Departamento de Engenharia Mecânica
Av. Brasil, 56 – Ilha Solteira/SP – CEP 18385-1000
Telefone: 18 3743.1000

ACKNOWLEDGEMENTS

I thank God for all the people who helped me on this journey to conquer this dream.

To my family and friends for their unconditional support at all times.

To my Professors for their educational support. In particular, to my advisor, Professor Leandro, for the teachings and friendship built over the last few years that have made me a better human and professional being.

ABSTRACT

The storage of CO_2 in underground reservoirs is a strategy currently used to mitigate the emission of greenhouse gases into the atmosphere, accelerating the development of new techniques for design of new equipments, obtaining technologies with higher global performances. The equipment studied in the present research is a centrifugal compressor operating with subcritical CO_2, in order to evaluate the influence of two splitters on the operational parameters of the rotor, which are isentropic efficiency, pressure ratio, required power and temperature ratio. The splitter geometrical parameters to be analyzed in the numerical simulation are the leading-edge position and the camber angles, which make up a total of 12 input parameters for a steady state, compressible, turbulent and three-dimensional flow. Coupled with CFD modeling, a promising approach to sensitivity analysis (SA) is associated with screening tools by the Morris' method, which is a low computational cost tool for 'factor fixation' allowing qualify the impact of the geometric parameters studied on the performance of the centrifugal compressor. The sensitivity analysis identified those geometric parameters that contribute significantly to the operating conditions of the centrifugal compressor. Specifically, the position of the leading and the trailing edge angles of the longer splitter are very influential on the four output variables and the hub angles of the shorter splitter have a relevant influence on the pressure ratio, required power and temperature ratio. Phenomenological analysis identified shock waves on the blade and the longer splitter, and a flow blocking region in the clearance gap. This reverse flow region is a significant source of loss, with an increase in static entropy of 62.9% in the second half of the impeller near the interface with the diffuser. The observed physical phenomena corroborate the ranking of the most important variables by the Morris method, proving to be a robust and effective tool in predicting the performance of centrifugal compressors.

LIST OF FIGURES

LIST OF TABLES

SUMMARY

1. INTRODUCTION

Industrial growth in the last decade combined with socioeconomic demands has changed the patterns of technological development in the world. As the number of industries increases, equipment and productive resources needs to be improved to expand production and reduce costs. Thus, several studies have emerged to investigate the efficiency of these industrial devices and improve production. Among the many types of equipment available in the industry, compressors have received special attention from the academic community and research and development centers. These are mechanical devices responsible for pressurizing the working fluid and delivering a higher pressure than the original pressure. Compression is used in many processes such as to provide air for combustion, transport process fluid through pipelines and provide compressed air for driving pneumatics tools [1].

The various industrial processes use different types of compressors according to the application, some of the most significant are centrifugal, axial, rotary and reciprocating compressors. The axial flow compressor is suitable for high flow rates and low-pressure rates, generally has higher efficiency, however, has a smaller operating region than a centrifugal machine. Rotary and reciprocating compressors (positive-displacement machines) are applied for low flow rates and high-pressure rates and the centrifugal compressor operates more efficiently at medium flow rates and high-pressure rates [1]. The centrifugal compressor, which is the focus of this research project, is the main compressor in the process of pipe industries, and, due to its compact size and comparable lightweight, it is widely used in the offshore industry [1]. The operating range of the mentioned compressors is presented in Figure 1 (1 CFM = 4.7x10^{-4} m^3/s).

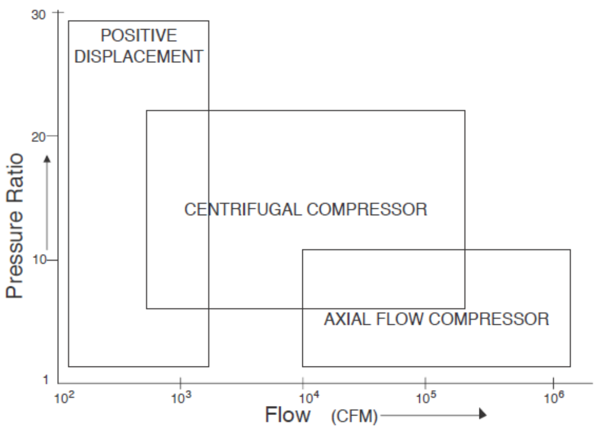

Figure 1 - Operating characteristics of different types of compressors [1].

Computational Fluid Dynamics (CFD) has been used more and more in several industry processes since it got mature as a powerful and reliable tool in industry and science, being used as much as experimental and analytical models to solve fluid flow problems [2]. Many packages and solvers had become cheaper in the past twenty years as CPU-power increased, allowing many applications of CFD techniques. For instance, in the complement of experimental data, providing a further comprehension of flow physical phenomena. Furthermore, it is considered an efficient tool for setting up experiments in the design of new equipment, allowing the implementation of optimization processes that are unfeasible through an experimental approach. [3].

1.1. Centrifugal Compressors Applied for CO_2 Storage

Currently, there is a notable increase in the concentration of greenhouse gases in the atmosphere, such as CO_2 and CH_4, contributing to the emergence of new strategies that make it possible to reverse this trend. With the increase in the concentration of these gases, climate changes are occurring and causing socioeconomic and ecosystem damage. The data presented by the Intergovernmental Panel on Climate Change (IPCC) [4] predicts that the global average temperature will rise by 3.5ºC by 2100. Among the actions that act to mitigate greenhouse gas emissions, capturing and storing CO_2 in underground reservoirs is a technological option that is gaining importance.

In the storage of CO_2 in underground reservoirs, several engineering processes are used to ensure the safe and long-term isolation of CO_2 from the atmosphere [5]. Depleted oil and gas reservoirs are the categories most likely to receive CO_2 from industrial processes and the process of CO_2 injection into existing oil fields is a technique known as "enhanced oil recovery" (EOR). It is estimated that 80% of reservoirs worldwide can be adapted for CO_2 injection [5]. Another alternative, the Enhanced Coal Ced Methane (ECBM) is also an option for storing CO_2 at infinite coal seams and has an additional benefit of methane production. [5]. The CO_2 capture and storage process consists of the removal of carbon dioxide from emissions resulting from industrial stationary sources, such as thermoelectric plants, cement plants, steel mills and petrochemical plants. Subsequently, CO_2 is compressed and transported through pipelines to the geological formation, as shown in Figure 2.

In the compression process up to the underground reservoirs, centrifugal compressors gain importance and the optimization of their geometry to obtain the ideal performance becomes essential. Numerous factors such as the working fluid itself, changing the operating specifications of compressors, adopting different strategies to satisfy the desired fluid characteristics after the compression process. In these applications, compressed CO_2 reaches a thermodynamic state with temperatures and pressures close to or above the critical point (supercritical CO_2), a region in which the transition between the liquid and gas phase is difficult to identify. The approach in this work will use the CO_2 below the critical point due to the observed instabilities in a supercritical fluid where small changes in pressure or temperature result in large changes in density.

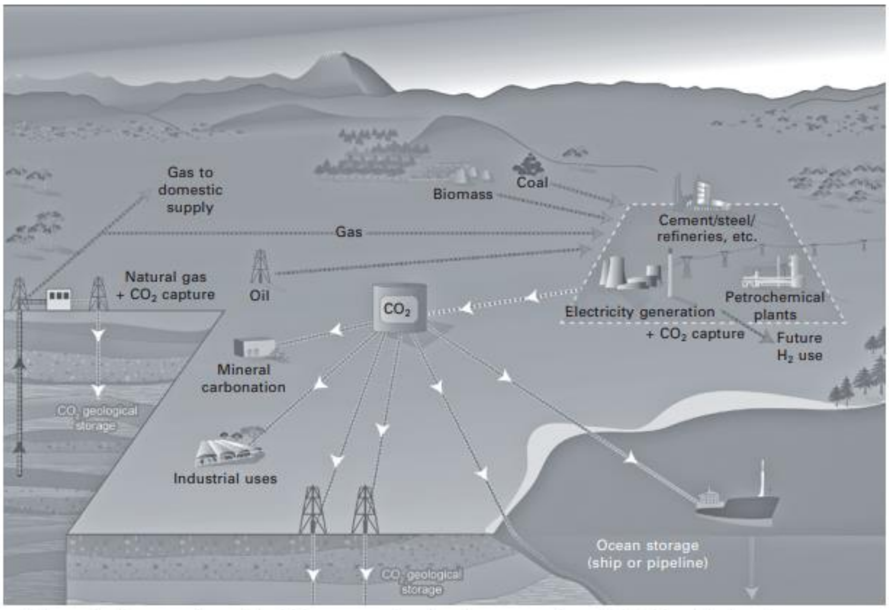

Figure 2 – CO_2 capture and storage in underground reservoirs [5].

1.2. Characteristics of CO_2 Centrifugal Compressor

Centrifugal compressors are fluid machines used to increase the pressure of gases [6]. As highlighted, they are employed in several industrial sectors such refineries, nuclear reactors and petrochemicals, because of their smooth operation of process fluctuation, and their higher reliability compared to other types of compressors [6]. Figure 3 shows the main parts of the centrifugal compressor. The impeller is responsible to transfer kinetic energy to the fluid, the diffuser to increase the fluid pressure and the volute smoothly discharges the flow [7]. In centrifugal compressors, a working fluid enters the compressor in an axial direction and exits in a radial direction into a diffuser. [8].

The study of geometric parameters that affect the performance of centrifugal compressors has been the focus of much academic research. Impeller, diffuser and volute, represented in Figure 3, are the components that present variations of changes in their geometry and have been widely studied in the optimization processes. In particular, in the impeller, the addition of splitters between the main blades has been investigated in the literature as an alteration capable of improving the pressure ratio and centrifugal compressor efficiency. The evaluation of the geometrical influence on centrifugal compressors has been possible from the vertiginous development of high-performance computers, which employ advanced numerical techniques to solve engineering problems.

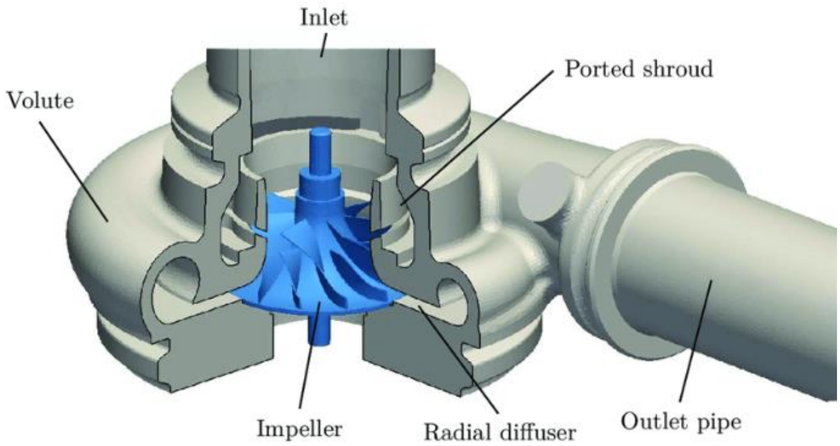

Figure 3 **-** Components of centrifugal compressors [9].

The impeller has two basic components, the inductor which is a radial flow rotor and the radial blades on which energy is transmitted by centrifugal force. Impeller blades have several geometric parameters that can be evaluated by centrifugal compressor optimization. It is composed of the trailing edge, leading-edge, and four surfaces, hub, shroud, suction, and pressure, as shown in Figure 4, which are much investigated in the literature [10]–[12].

The diffusers can be classified as vaned or vaneless. They are designed to convert the high velocity exiting from the impeller to static pressure. Diffusing passages have always played a vital role in obtaining good performance from turbomachines [1]. Their role is to recover the maximum possible kinetic energy leaving the impeller with a minimum loss in total pressure. The velocity of the fluid is converted to pressure, partially in the impeller and partially in the stationary diffusers. In this work, the vaneless diffuser was used to assist in the implementation of the model.

The volute is used to collect the flow from a vaned or vaneless diffuser and to guide it out of the compressor. The volute geometry is usually designed based on a certain rotational speed and mass flow rate in order to get a constant flow in the design point. This also means a constant static pressure distribution in the circumferential direction. The final component downstream of the scroll is the conical diffuser, often regarded as an integral part thereof, connecting the scroll exit to the discharge nozzle [6].

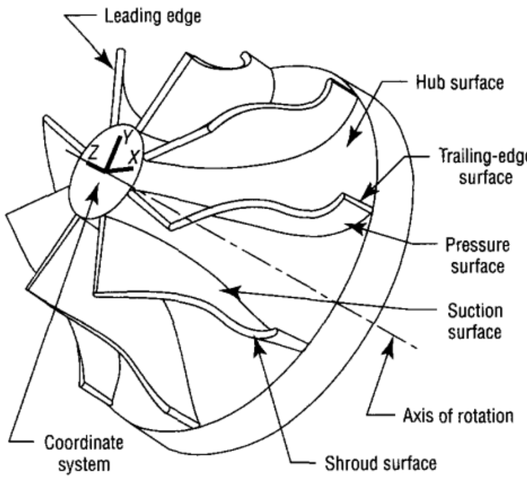

Figure 4 - Impeller geometrical parameters [13].

1.3. Splitters

In the design of centrifugal compressor impeller blades, some factors that alter fluid flow have led to modifications in its geometry that are applied commercially and in designs. Among these changes is the addition of smaller sized blades known as splitters. Splitters are used to increase the pressure ratio and minimize the effects of blocking fluid flow at the leading edge of the main blades. Oana *et al* [14] performed the optimization of a centrifugal compressor by equalizing the flow on both sides of the splitters and reported some efficiency improvements. Lohmberg *et al* [15] investigated the effects of splitter addition and identified that their proper positioning would prevent blockage of the flow passage at the inlet. Michelassi [16] studied the impact of forward and aft sweep on the main and splitter blade leading edge of a generic high flow coefficient and high-pressure ratio centrifugal compressor design and the impact on its overall peak efficiency, pressure ratio and operating range. The studies conducted on the splitter leading edge profile indicate that aft sweep may help to increase the operating range of the impeller analyzed by up to 16% while maintaining similar pressure ratio and efficiency characteristics of the impeller. The impeller with the addition of splitters is shown in Figure 5.

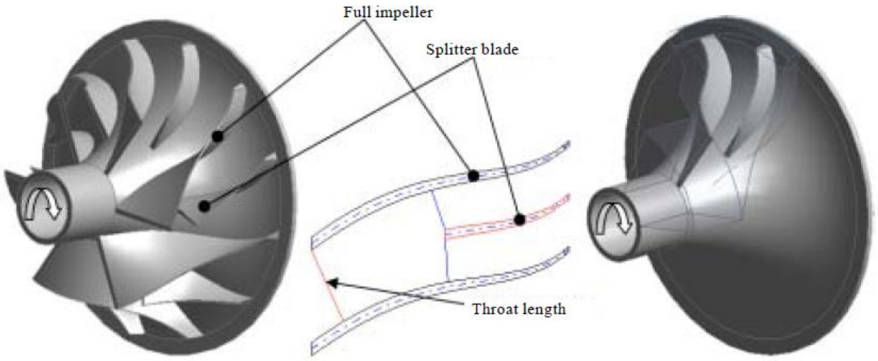

Figure 5 - Impeller with the addition of splitters [17].

The traditional approach uses a splitter interspersed with the main blades. Moussavi *et al* [12] investigated the effect of changes in splitters leading-edge position and angle, while the blade profiles and impeller dimensions of the standard compressor were unchanged. With the implementation using genetic algorithm and CFD codes, they found an optimized configuration for the centrifugal compressor that demonstrated a 5% reduction in impeller inertia. Another approach is to use multisplitters in the centrifugal impeller. Malik *et al* [18] performed impeller optimization by adding a big splitter close to the pressure surface and a small splitter close to the suction surface. They reported that the introduction of multi-splitters reduced flow separation, increased pressure ratio from 4.1 to 4.5 and promoted a 2% increase in impeller efficiency. The multiple splitter impeller is shown in Figure 6.

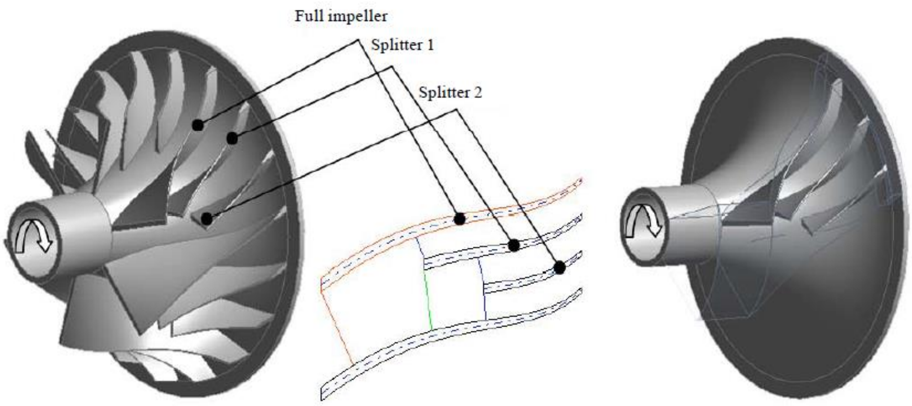

Figure 6 - Impeller with the addition of multisplitters [17].

The main goal of the present research project is to identify the impact of the introduction of two splitters on centrifugal compressor performance by characterizing the patterns of impeller flow dynamics. The position study of the leading edge and the camber angles of two splitters added to the impeller are the geometric parameters evaluated in the numerical simulation and submitted to a sensitivity analysis methodology in order to identify their influence on possible impeller improvements. Understanding the main phenomena that involve the flow in the centrifugal compressor allows extrapolating the ideal geometric configuration that increases the efficiency of these types of equipment, enabling its implementation in the industry.

2. METHODOLOGY

2.1. CO_2 Centrifugal Compressor

The initial geometry of the impeller (blade + 1 splitters) will be generated in ANSYS Vista CCD. The ANSYS Vista CCD is a tool based on one-dimensional calculations and empirical correlations to facilitate the construction of different blade models for turbomachinery. The input data required in Vista CCD are divided in operational data, gas properties and geometry. The operational data contains pressure ratio, mass flow, rotational speed, inlet pressure and temperature. The gas properties are related to the fluid model, which is available for a shortlist of substances, including the gas model for CO_2. Finally, geometrical constraints are required as hub diameter, vane normal thickness, leading-edge angle of inclination, clearance gap distance, among others. Table 1 summarizes the main boundary conditions applied to the pre-processing setup (ANSYS Vista CCD) and some geometrical features of the rotor.

Table 1 - Boundary conditions and geometrical features.

Rotation velocity	12500 rpm
Mass flux	55.56 kg/s
Inlet pressure	400 kPa
Inlet temperature	320 K
Inlet turbulence	5%
Clearance gap	1 mm
Wall condition	No-slip
Roughness	Smooth
Number of blades	10
Number of splitters	10
Impeller exit diameter	529.3mm

Source: Author, (2024).

Following three possible correlations: Casey-Robinson [19], Casey-Marty [20] and Rodgers [21], Vista CCD provides a “base efficiency” compressor map that is used to generate a blade geometry profile that satisfies the pre-imposed conditions. Among these possibilities, the

Casey-Robinson correlation was used to predict the performance map of the centrifugal compressor. The calculation of the variables polytropic efficiency and work coefficient for the flow coefficient and tip-speed Mach number are parameters that help to identify the applicability of the model for the desired operating conditions. A meridional view of the impeller blade and its efficiency map is presented in Figure 7.

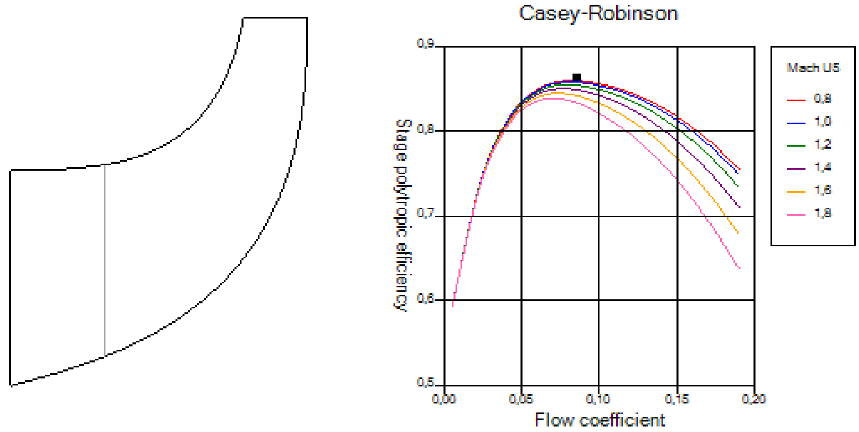

Figure 7 - Vista CCD blade sketch and impeller efficiency map (Author, 2024).

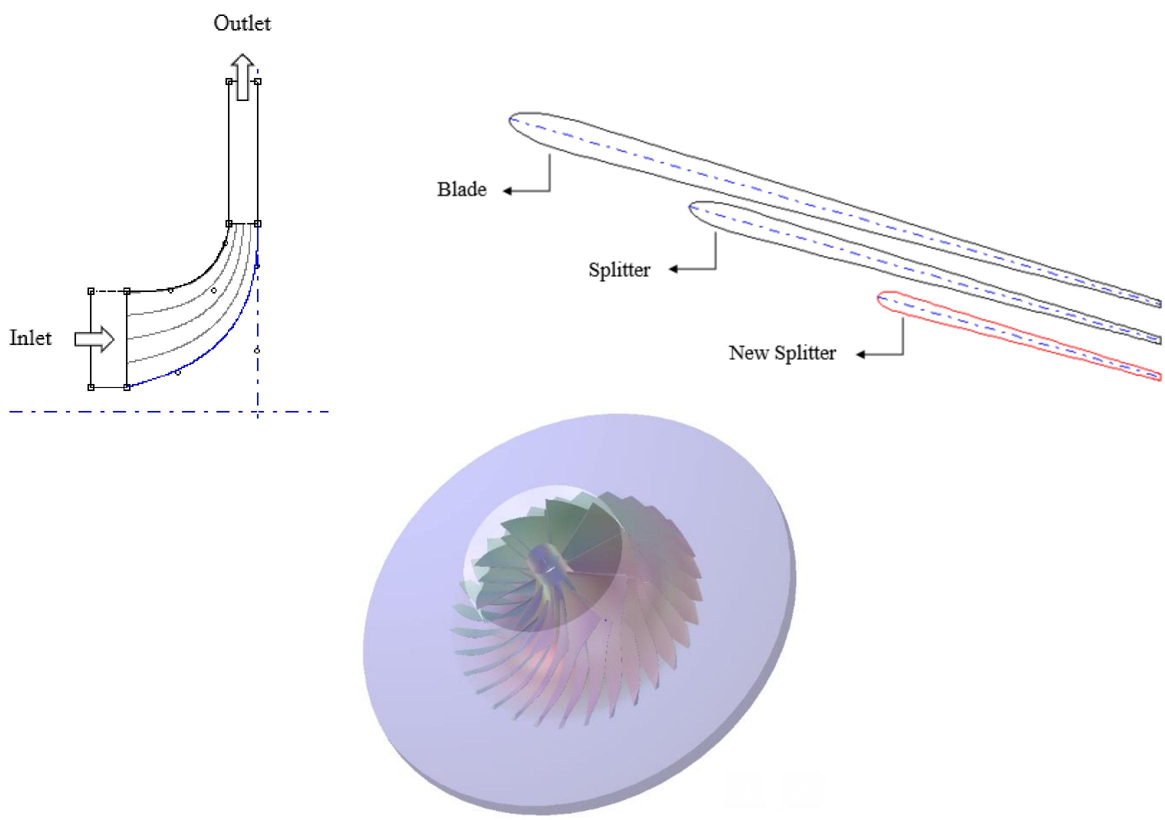

Figure 8 - Geometry generated in BladeGen + Vista CCD (Author,2024).

The ANSYS Vista CCD makes it possible to add only one splitter (intervane) to the geometry. Through BladeGen, a new splitter was created and some adjustments in the inlet and outlet of the fluid domain were made to obtain a consistent model. The splitters and blades were defined with equal spacing on the trailing edge. Other parameters such as thickness and number of layers were set as default those generated by Vista CCD. Initially, the position of the leading edge of the splitters and the splitters camber angles were arbitrary, as they will be evaluated in detail during parameterization. Figure 8 shows the geometry generated in BladeGen + Vista CCD.

2.2. Geometrical Parametrization

The geometric parameterization was performed in ANSYS Design Modeler from the geometry generated in Vista CCD + BladeGen. This process will be divided into two main stages: meridional shape and angles. To obtain the meridional parameterization of the shape, eight control points were determined as limiting points of the fluid passage domain shown in Figure 9, in which points P4 and P8 are representative for the blade and splitters. Note that the orange and green lines constitute the leading edge of the blade and the trailing edge of the blade and splitters, respectively. The black and purple lines represent the leading edge of splitters, while the other lines represent the fluid passage domain. Points P1, P4, P5, and P8 have been fixed to the x and z axes to ensure proper blade and separator shape while the remaining points are free on the z axis and follow the contour of the hub and shroud. Therefore, 4 input parameters are defined.. Therefore, 4 input parameters are set.

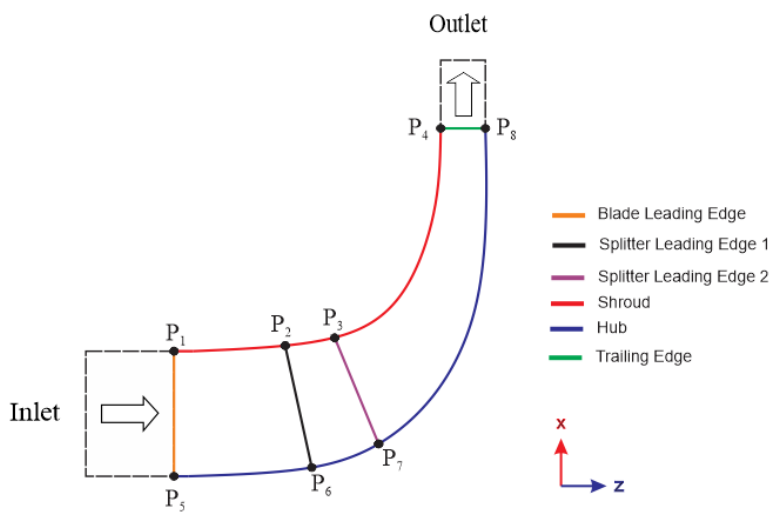

Figure 9 - Centrifugal Compressor Impeller Meridional View (Author, 2024).

To acquire the parameterization of the splitters camber angles, two layers corresponding to the hub and shroud of this geometry were created in the meridional plane. Two points are defined on each layer in a curve that represents the camber angle as a function of chord distance, as shown in Figure 10.

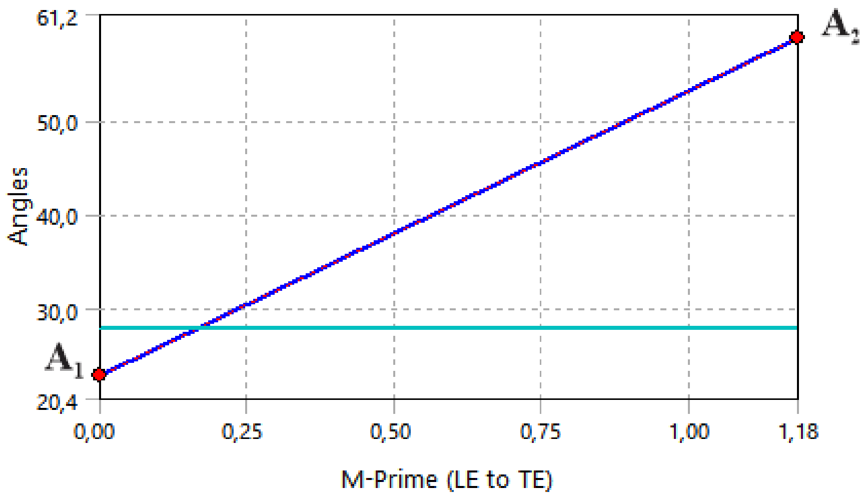

Figure 10 - Angle parametrization (Author,2024).

Points A1 and A2 are fixed at the beginning and end of the splitter blade along the x-axis and free along the y-axis. Therefore, two parameters for each meridional layer are defined, resulting in 4 additional input parameters for each splitter. The thickness of the splitters and the blade as well as the distance between them will be fixed. Thus, the parameterization has an amount of 12 input parameters that will be analyzed during the sensitivity analysis procedure. Table 2 summarizes the parameterized input variables for the two splitters.The final parameterized geometry is shown in Figure 11.

Table 2 – Input variables.

	Layer	**Leading Edge Position**	**Leading Edge Angles**	**Trailing Edge Angles**
Splitter 1	**Hub**	P6	A6	A81
	Shroud	P2	A2	A41
Splitter 2	**Hub**	P7	A7	A82
	Shroud	P3	A3	A42

Source: Author, (2024).

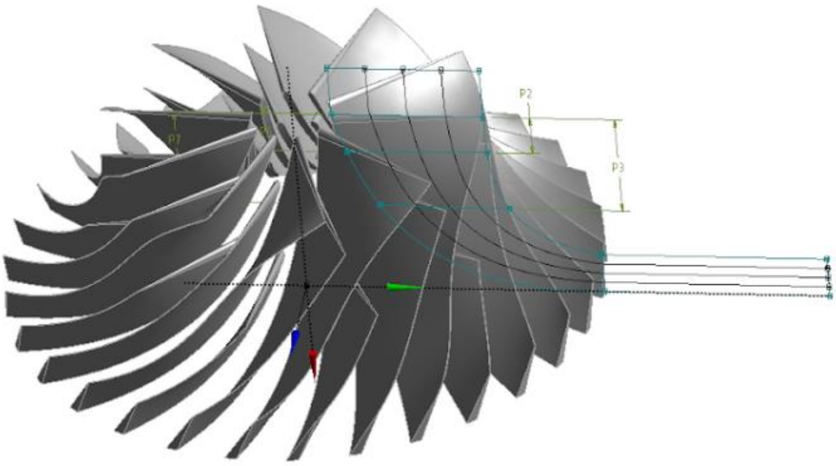

Figure 11 - Parameterized geometry (Author,2024).

2.3. Grid Generation and Computational Domain

The parameterized geometry in ANSYS Design Modeler was imported for meshing in Turbogrid, which is a specialized tool that develops grids for turbomachinery, which provides relatively fast mesh construction. It discretizes the periodical domain with attention to some important quality criteria as y+. The project uses the SST turbulence model and to satisfy the conditions, y+ below 10 was defined as one of the criteria for generating the mesh, with the insertion of the number of Reynolds equal to $5x10^7$, which characterizes the flow inside the centrifugal compressor. In topic 3.1 the results found will be discussed.

ANSYS Turbogrid provides practical and immediate information about the quality of the mesh, highlighting criteria such as grid skew angles, mesh expansion rates, and aspect ratios of mesh elements. The elements that do not meet the quality criteria are highlighted in red, identifying the necessary corrections that must be made in the mesh generation control. Figure 12 shows the mesh constructed for the model of the present work.

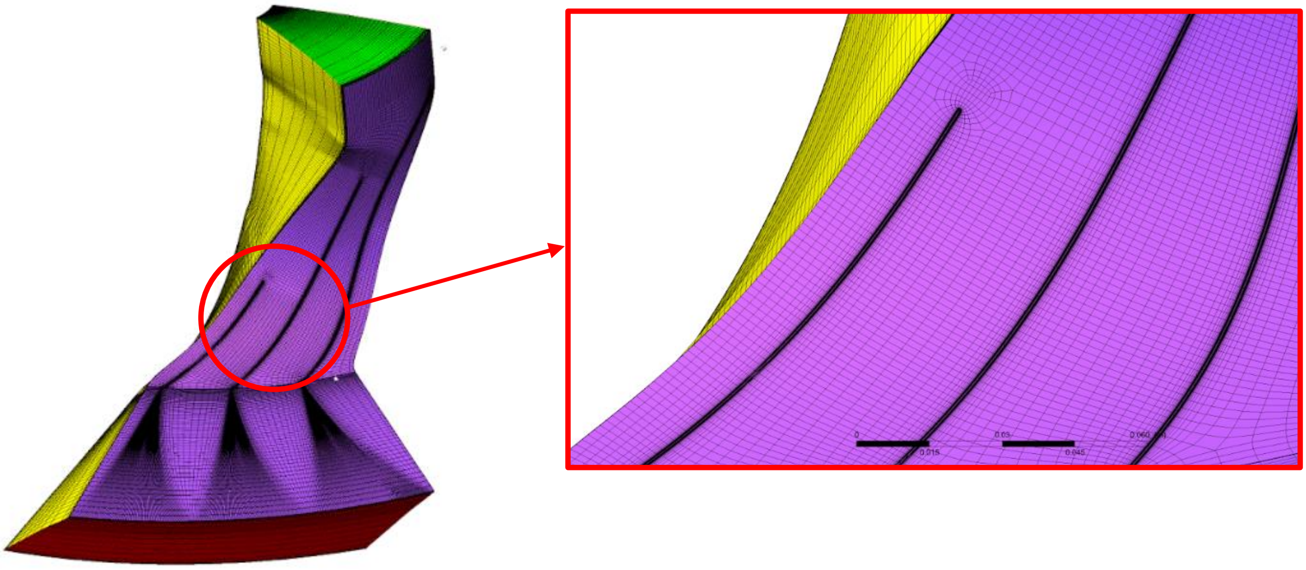

Figure 12 - Details of the mesh generated in the Turbogrid (Author,2024).

Figure 13 shows the impeller/vaneless diffuser geometry, highlighting the periodical computational domain that is used to reduce the computational time of a full-sized impeller. The equivalence theorem uses the symmetric parts (periodical domain) of the whole as they are considered to have the same behavior. The solution of only a single part is extrapolated to the others, given the complete solution at a lower computational cost.

Impeller + Vaneless Diffuser **Periodical Computational Domain**

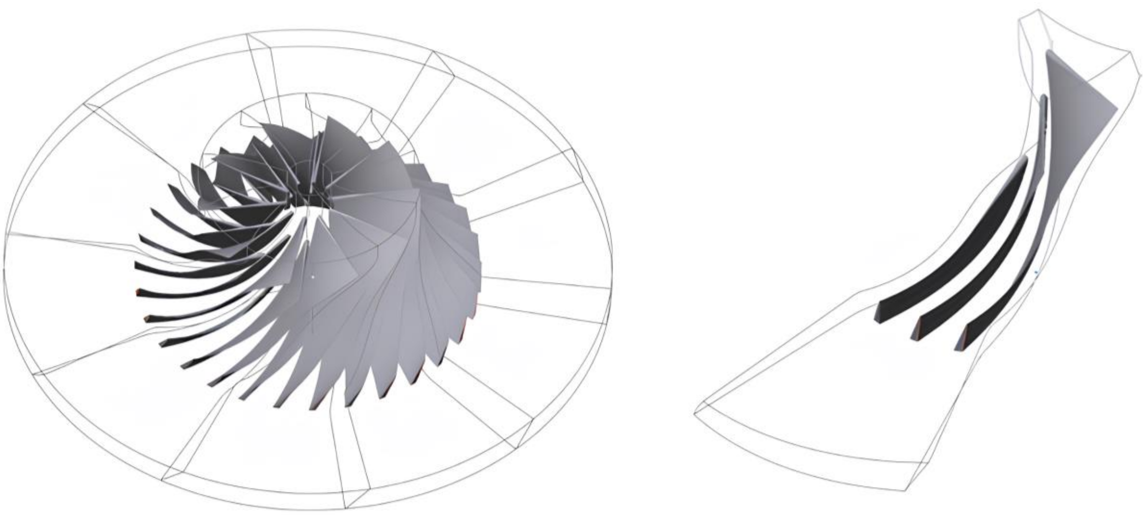

Figure 13 - Geometry impeller + vaneless diffuser model (Author,2024).

2.4. Numerical Simulation

Benini et al., [22] suggest the use of a steady-state flow model for impellers since the fluctuations in the flow of a centrifugal compressor are important only at the impeller vanned-diffuser gap, which is not present in an impeller vaneless-diffuser evaluated herein. Furthermore, the flow is highly turbulent and three-dimensional using CO_2 as a working fluid modeled by Redlich-Kwong for a real gas equation of state modified by Aungier [23]. Hence, the analysis considers a steady-state flow for a real gas, compressible, turbulent and tridimensional flow, in a periodical computational domain. The computational domain and its boundaries are shown in Figure 14 and detailed in Table 3.

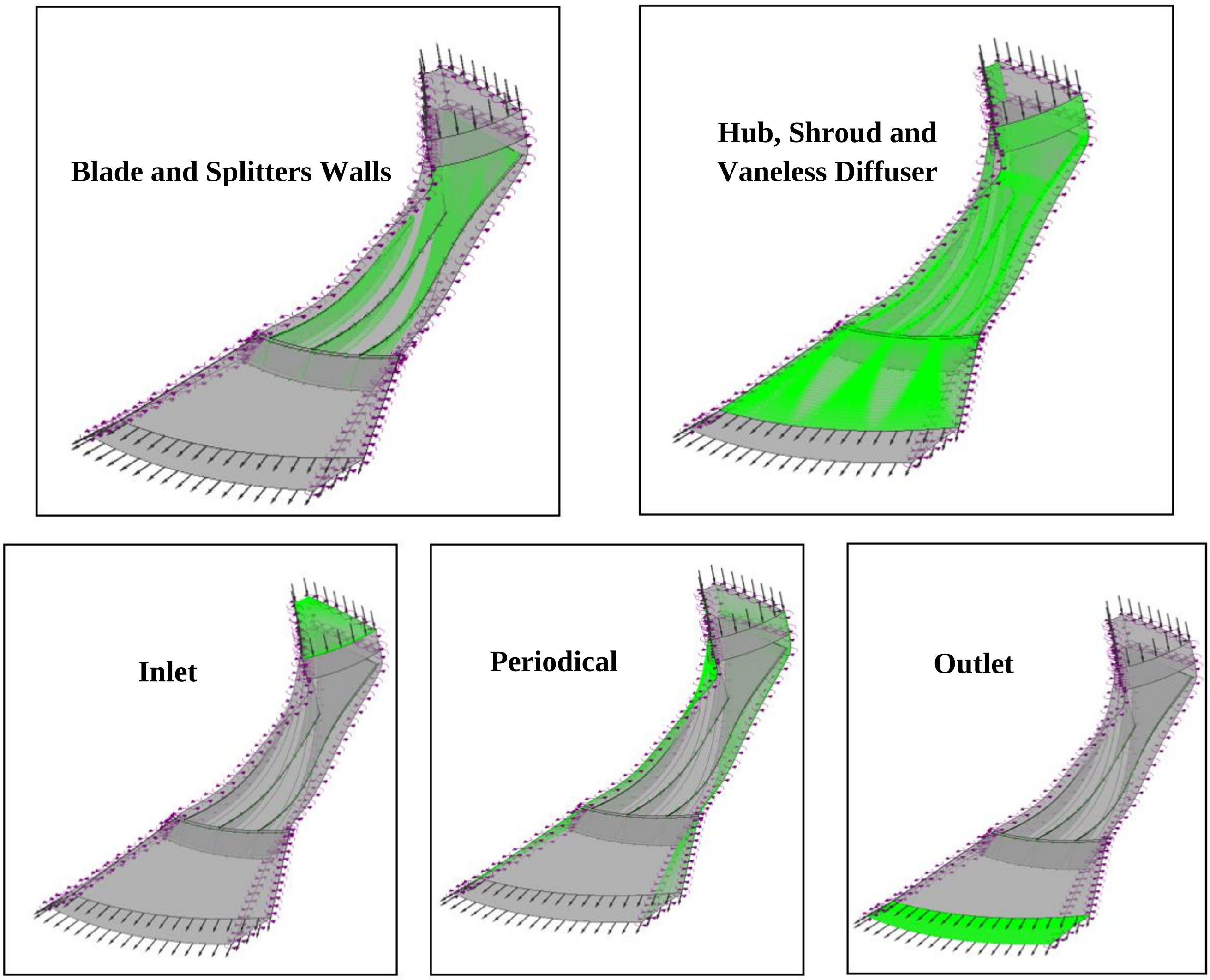

Figure 14 - Boundaries conditions on the periodical computational domain (Author,2024).

Table 3 - Boundary conditions on the computational domain.

Boundary	**Conditions**
Blade and splitters walls, hub, shroud and vaneless diffuser	No slip; Smooth Wall; Adiabatic.
Inlet	Relative Pressure (400 kPa); Turbulence Intensity; Fixed temperature (320 K).
Outlet	Fixed mass flow rate (55.56 kg/s).
Periodical	Conservative Interface Flux.

Source: Author, (2024).

The ANSYS CFX is recognized to be expert software in applications of turbomachinery and it was selected to conduct this study. It imports the mesh from ANSYS Turbogrid, sets the boundary conditions and solves the seven physical model governing equations presented below:

- Continuity:

$$\nabla \cdot (\rho \boldsymbol{U}) = 0 \tag{1}$$

- Momentum (3 equations):

$$\nabla \cdot (\rho \boldsymbol{U} \times \boldsymbol{U}) = -\nabla \mathrm{p} + \nabla \cdot \tau + S_M \tag{2}$$

where τ is the stress tensor and accordingly to the rotating frame of reference equations of ANSYS CFX®: $S_M = S_{M,rot} = S_{cor} + S_{cfg}$. In which $S_{cor} = -2\rho\ (\omega \times \boldsymbol{U})$ (Coriolis Force) and $S_{cfg} = -\rho\ \omega \times (\ \omega \times \boldsymbol{r})$ (Centrifugal Force).

- Total Energy:

$$\nabla \cdot (\rho \boldsymbol{U}\boldsymbol{I}) = \nabla \cdot (\lambda \nabla \mathrm{T}) + \nabla \cdot (\boldsymbol{U} \cdot \tau) + \mathbf{U} \cdot \boldsymbol{S_M} + S_E \tag{3}$$

Where the rothalpy is $\boldsymbol{I} = h_{stat} + \frac{\mathbf{1}}{\mathbf{2}}(U^{\mathbf{2}} - \ \omega^{\mathbf{2}})R^{\mathbf{2}}$.

- k-ω SST turbulence model (2 equations):

$$\frac{\partial(\rho U_j k)}{\partial x_j} = \frac{\partial[(\mu+\frac{\mu_T}{\sigma_k})\frac{\partial k}{\partial x_j}]}{\partial x_j} + P_k - \beta' \rho k \omega + P_{kb} \tag{4}$$

$$\frac{\partial(\rho U_j \omega)}{\partial x_j} = \frac{\partial[(\mu+\frac{\mu_T}{\sigma_\omega})\frac{\partial \omega}{\partial x_j}]}{\partial x_j} + \alpha \frac{\omega}{k} P_k - \beta \rho \omega^2 + P_{\omega b} \tag{5}$$

where the production term has been modified accordingly to [24], to better fit the streamline curvature and rotational system.

In order to evaluate the grid density independence, the Grid Convergence Index Method (GCI) is known as a robust method [19]. This method is based on Richardson's extrapolation, capable of measuring the discretization error of the computational domain, validated for several hundred CFD cases. The application of this methodology compares three mesh densities, with refinement factors r, greater than 1.3, as recommended by Celik et al.[25], and has as input parameters the number of cells and the sum of their volumes. Thus, it is possible to define the representative cell size, h, which is calculated for the three grids considering the three-dimensional modeling.

$$h = \left[\frac{1}{N}\sum_{i=1}^{N}(\Delta V_i)\right]^{1/3} \tag{6}$$

In which ΔV_i is the volume of the i-ésimo and N is the total number of cells.

The grid refinement factor defined is:

$$r = (\frac{n_{n+1}}{n_n})^{\frac{1}{3}} > 1.3 \tag{7}$$

where n_{n+1} is the number of elements of the refined mesh and n_n the number of elements in the coarse mesh.

2.5. Sensitivity Analysis Methods

Sensitivity Analysis is a tool used in engineering projects to evaluate the impact of variations in parameters in a model and assist in decision making. The centrifugal compressor is equipment that goes through geometric optimization processes to improve operational performance and has a high range of possible input variables to be analyzed. Associated with CFD modeling, sensitivity analysis makes it possible to reliably and robustly identify the main influential parameters and reduce the number of parameters subject to the optimization process, reducing computational costs.

2.5.1. The Elementary Effects Method

The elementary effects (EE) method was developed by Morris [26] and the proposal is to select the input factors that are important for a model among the various factors that can be evaluated. The sensitivity analysis proposed by Morris classifies the effects of input factors as (a) insignificant, (b) linear and additive, or (c) nonlinear or involved in interactions with other factors [27]. Considering a model with *k* independent inputs X_i, (i = 1,…,k). For a given value of X, the Elementary Effect is defined as:

$$EE_i = \frac{[Y(X_1,X_2,\ldots,X_{i-1},X_i+\Delta,\ldots,X_k)-Y(X_1,X_2,\ldots,X_k)]}{\Delta} \qquad (8)$$

Where Δ is the step in the discretized input space. For a more efficient design, Morris [26] suggested the construction of r trajectories of (k+1) points in the input space, with a total cost of the experiment equal to r(k+1).

The Morris method proposes two sensitivity measures to classify input variables: μ (mean of each EE distribution that evaluates the global influence of the variable) and σ (standard deviation of each EE distribution that estimates the influence on interactions with other factors) [27]. These measures are defined as follows.

$$\mu_i = \frac{1}{r}\sum_{j=1}^{r} EE_i^j \tag{9}$$

$$\sigma_i^2 = \frac{1}{r-1}\sum_{j=1}^{r}(EE_i^j - \mu_i)^2 \tag{10}$$

Campolongo et al. [28] proposed an improvement in the calculation of mean μ to solve the problem of elementary effects with opposite signs in a non-monotonic model and which may fail to identify an important factor. The suggested revision is to calculate the mean of the distribution with absolute values of the elementary effects, known as μ*:

$$\mu_i^* = \frac{1}{r}\sum_{j=1}^{r} |EE_i^j| \tag{11}$$

Campolongo et al. [29] adopted a method to increase input space coverage, especially for models with a large number of input factors. The improvement is in the sampling strategy, scanning the input domain without increasing the number of model runs required. The proposal is to select the trajectories *r* maximizing the dispersion in the input space. A high number of trajectories are generated (M=500-100) and those with the largest 'spread' are selected based on the following distance d_{ml} definition:

$$d_{ml} = \begin{cases} \sum_{i=1}^{k+1}\sum_{j=1}^{k+1}\sqrt{\sum_{z=1}^{k}[X_i^m(z) - X_j^l(z)]^2} & for\ m \neq l \\ 0 & otherwise \end{cases} \tag{12}$$

Where m and l are the analyzed trajectories, k is the number of input factors and $X_i^m(z)$ indicates the z^{th} coordinate of the i^{th} point of the m^{th} Morris trajectory[30]. The quantity D is calculated for all possible combinations of trajectories r and those with the highest value are selected.

Input variables need to be classified to determine effects on the model. Vanrolleghem et al. [31] suggested a terminology to classify variables as important/non-important and influential/non-influential using the EE method with the definition of a cut-off threshold. Thus, it is possible to identify the behavior of the variables in relation to the absolute mean (μ*) and standard deviation (σ). In Figure 15, the line corresponding to $\mu_i^* = 2SEM_i$, where SEMi ($\sigma_i r^{-\frac{1}{2}}$) represents the standard error of the mean, is used for establishing the type of effect of variables [26]. Variables which lie outside the wedge formed by the line corresponding to the established CT_{MORRIS} and the line $\mu_i^* = 2SEM_i$ have a linear effect on the model outputs and and those that are inside the area, have a non-linear effect [31].

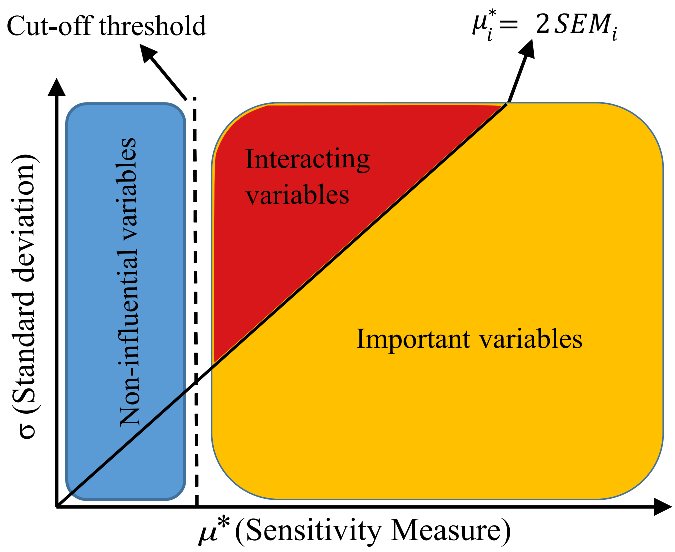

Figure 15 - Differentiation of variables in Morris Screening Method [31].

2.6. Grid Convergence Index (GCI)

The study of mesh independence is essential to ensure the validity of the numerical modeling. The isentropic efficiency, pressure ratio, required power and the temperature ratio are the variables that most affect the performance of turbomachinery and must be evaluated in the GCI [25]. The results for the current modeling are shown in Table 4.

Table 4 - GCI results.

Model Grid	Cells number	Refinement factor	Isentropic Efficiency (%)	Pressure Ratio	Temperature Ratio	Power Required (MW)
Coarse	1.943×10^6	-	81.55	3.17	1.335	5.30
Medium	4.358×10^6	1.31	80.32	3.12	1.335	5.31
Fine	9.487×10^6	1.30	80.19	3.12	1.337	5.32
GCI (%)	**-**	**-**	**0.027**	**0.024**	**0.018**	**0.133**

Source: Author, (2024).

The GCI results demonstrate low values of numerical uncertainty on the evaluated parameters and, therefore, the independence of the grid was achieved, proving that the average grid is acceptable for the continuity of numerical simulations.

2.7. Numerical Validation

As there is a lack of experimental data regarding this work operational conditions for the CO_2 centrifugal compressor, Casey and Robinson's one-dimensional approach was used for validation purposes. Their 1D streamline curvature method [32] has demonstrated extremely good agreement with 3D CFD (ANSYS CFX) and their efficiency prediction equations [19] were consistent with more than 45 different compressor stages with typical efficiency errors in the range of ± 2%. They argue that their method uses non-dimensional performance coefficients and specific experimental data, so it can be adapted to several gases and applications. Table 5 presents the results of Casey and Robinson equations predictions by ANSYS VISTA CCD software compared to ANSYS CFX medium grid results.

As can be seen in Table 5, the 3D CFD results are quite similar to VISTA CCD [18,28], with low percentage differences for isentropic efficiency, pressure ratio and required power, which are the main parameters analyzed in the present study. Therefore, the results obtained are sufficient for the numerical validation of the model.

Table 5 - Numerical validation.

Model	**Isentropic Efficiency (%)**	**Pressure Ratio**	**Power Required (MW)**
Medium Grid (Present Work)	82.92	2.80	4.62
VISTA CCD	82.40	2.85	4.71
Error (%)	**0.52**	**1.75**	**1.91**

Source: Author, (2024).

3. RESULTS AND DISCUSSION

3.1. Mesh Quality

To obtain stability and precision of the numerical simulation results, some quality parameters of the mesh generated in the TurboGrid must be satisfied. Four criteria to ensure mesh quality are suggested by CFX Theory Guide [33]: orthogonal angle, expansion factor, aspect ratio and y^+. The values of the orthogonal angle and expansion factor are in accordance with the specifications. A detailed analysis of the mesh showed that 7.3% of the cells have an aspect ratio well above that recommended (1000). However, these low-quality cells did not affect the numerical simulation, which presented consistent results and convergence, as shown in Figure 16.

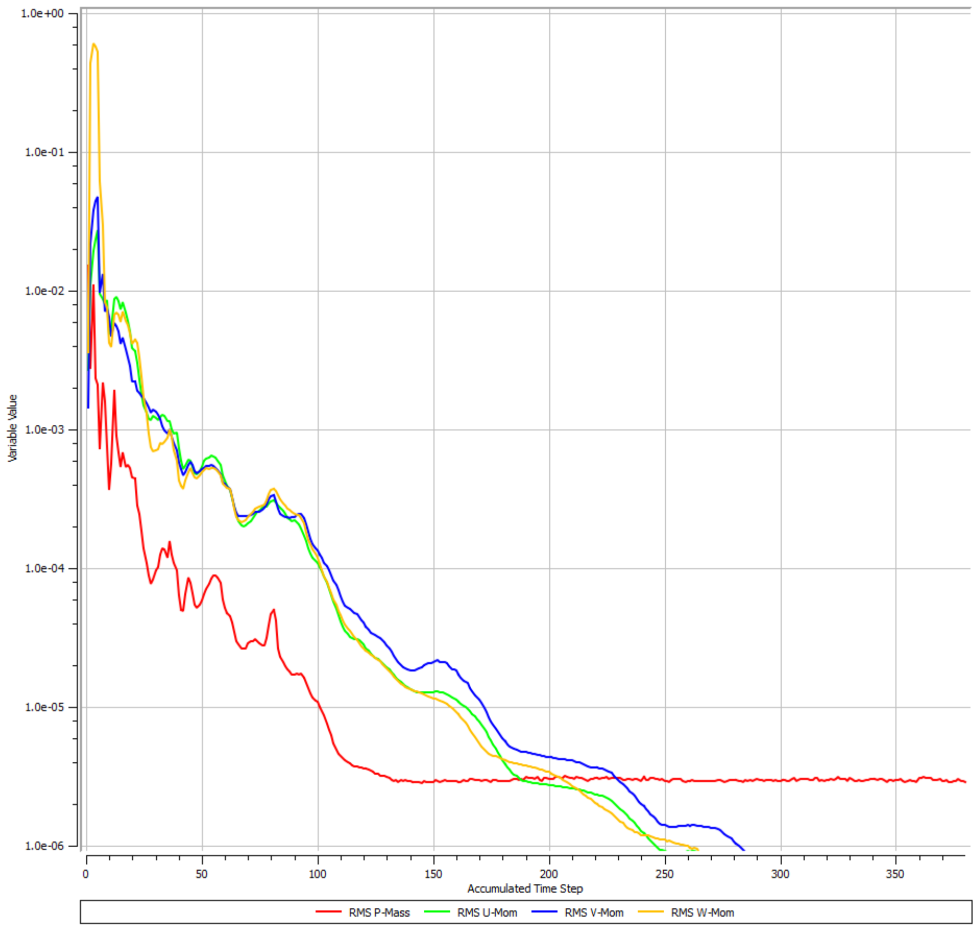

Figure 16 - Residuals convergence, medium grid (Author,2024).

An automatic near-wall treatment applied in regions where the value of y^+ is greater than unit was implemented by Menter and Knopp [34], [35]. They claim that these equations help the turbulence model to find accurate results even with the condition of low near-wall distance not being fulfilled. Their approach suggests the results are reliable for values of y^+ up to about 10 for the k-ω SST turbulence model. An evaluation of the impeller/vaneless diffuser found that 4.2% of the cells are y^+ higher than 10, concentrating at the interface between these two components, as shown in Figure 17. These values are within acceptable limits, which can be considered satisfactory for the model of this work.

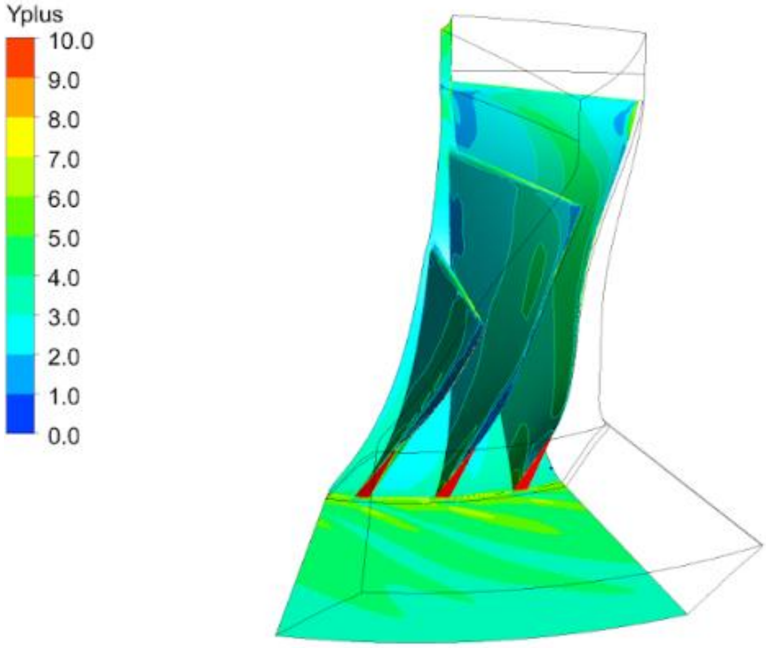

Figure 17 - $\boldsymbol{y^+}$ quality criteria for k-ω SST – turbulence model (Author,2024).

3.2. Morris' Sensitivity Analysis

With the numerical validation of the model, it is possible to proceed to the next steps of the project, with the development of sensitivity analysis through the implementation of the Morris method in software R. Table 6 shows the original (defined by ANSYS VISTA CCD and BladeGen), lower and upper values of the input variables. The range of input variables was defined according to the geometric limitations generated by changing the leading edge and camber angles of the splitters and the quality of the mesh obtained to avoid numerical divergence.

Table 6 - Input variables range.

	Leading Edge (mm)				**Angles (Degrees)**							
Variable	**P2**	**P3**	**P6**	**P7**	**A2**	**A3**	**A41**	**A42**	**A6**	**A7**	**A81**	**A82**
Lower	30	95	30	95	-1	-1	37	19	-3	0	40	25
Original	38.0	98.2	40.1	96.6	2.2	2.2	39.1	21.4	0	0.5	42.3	26.4
Upper	50	115	50	115	3	3	40	23	1	3	44	29

Source: Author, (2024).

In order to assess the overall performance of a centrifugal compressor, four important parameters have been considered: isentropic efficiency, pressure ratio, required power and temperature ratio. A suitable project of a compressor should seek the highest isentropic efficiency and pressure ratio with the lowest required power and temperature ratio as possible. Therefore, these variables were chosen as the interest outputs of this study. Figures 18 shows the histograms of the Morris' for the main effects for each input variable considering the interest outputs. The ranking histograms were achieved by running 130 CFD cases (r(k+1)). Table 7 presents the ranges of the output variables obtained in the numerical simulations.

Table 7 - DoE Analysis.

	Isentropic Efficiency (%)	**Pressure Ratio**	**Power Required (MW)**	**Temperature Ratio**
Range	78.60 to 83.04	2.98 to 3.22	5.09 to 5.32	1.32 to 1.34
Difference (%)	**4.44**	**8.05**	**4.50**	**1.30**

Source: Author, (2024).

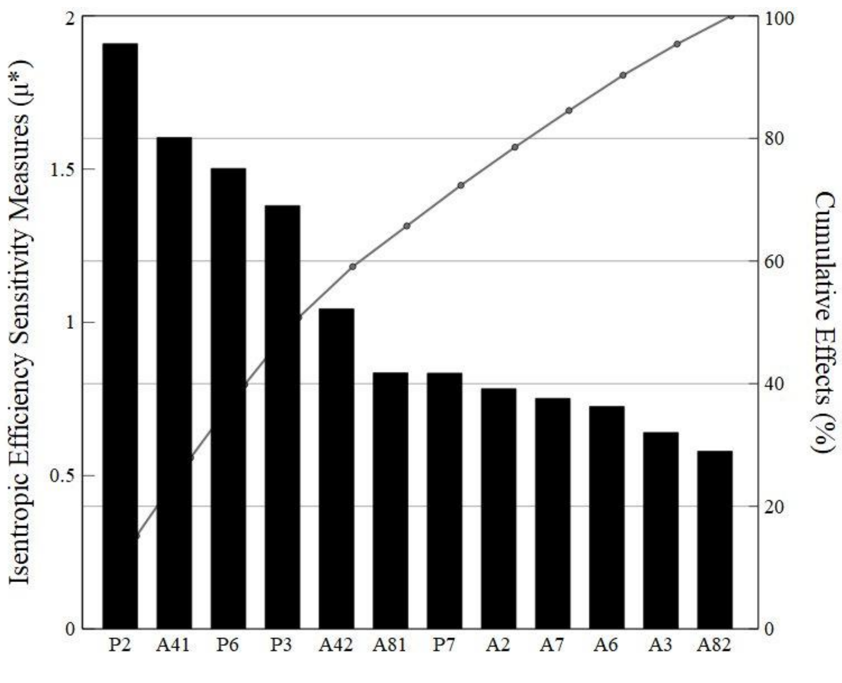

(a)

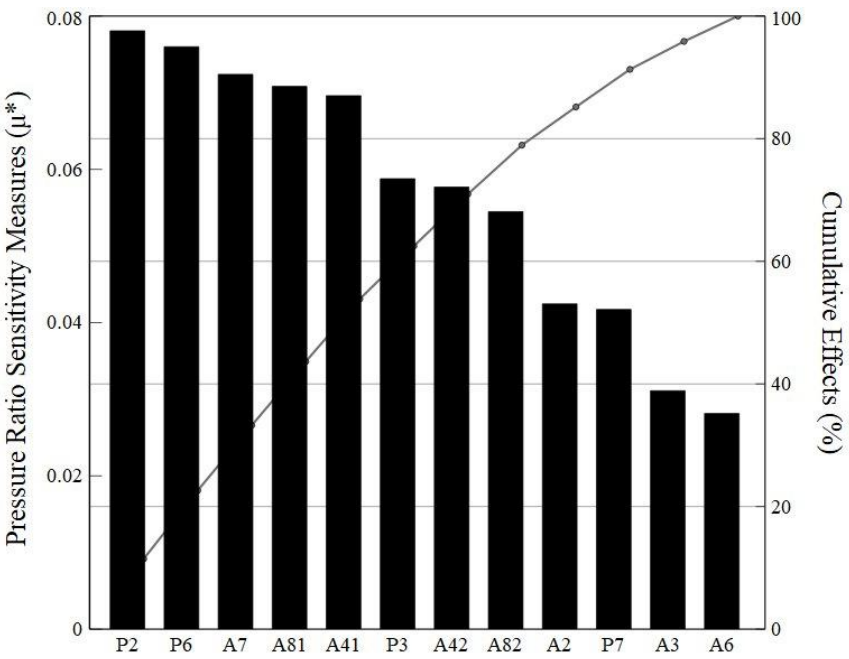

Pressure Ratio Sensitivity Measures (μ*)
Cumulative Effects (%)
0.08
0.06
0.04
0.02
0
100
80
60
40
20
0
P2
P6
A7
A81
A41
P3
A42
A82
A2
P7
A3
A6

(b)

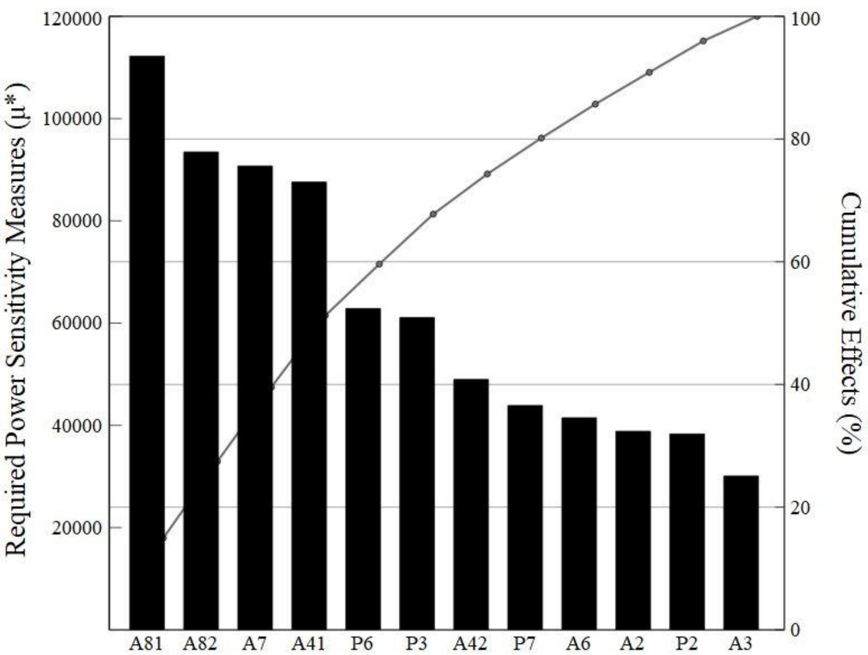

Required Power Sensitivity Measures (μ*)
Cumulative Effects (%)
120000
100000
80000
60000
40000
20000
100
80
60
40
20
0
A81
A82
A7
A41
P6
P3
A42
P7
A6
A2
P2
A3

(c)

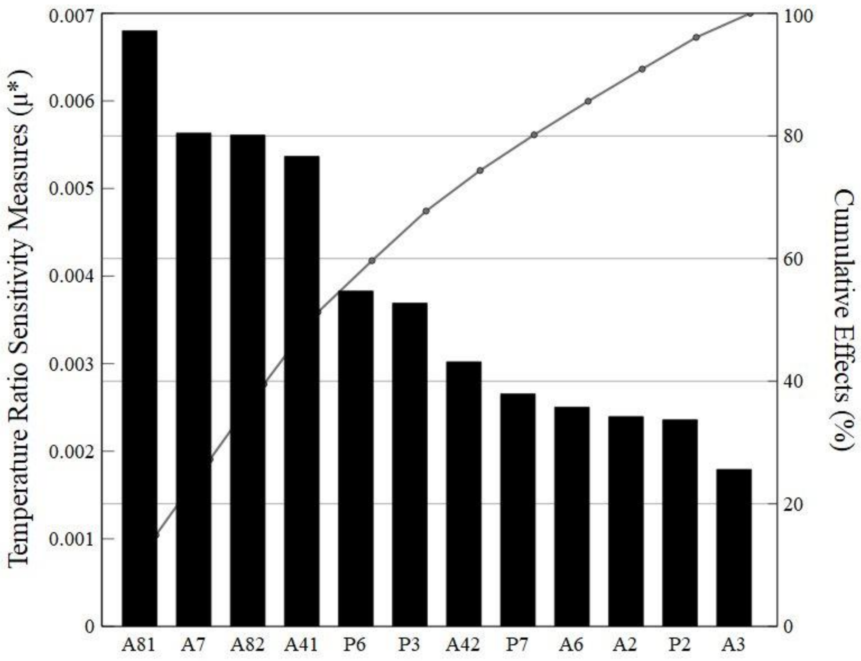

(d)

Figure 18 - Main effects sensitivity measures of Morris Screening method; (a) isentropic efficiency, (b) pressure ratio, (c) required power and (d) temperature ratio (Author,2024).

The cumulative effect curve of the absolute mean (μ*) demonstrated that the input variables had a significant impact on the evaluated output parameters. The variable P2 corresponding to the leadind edge position on splitter 1 (longer) was the most influential for isentropic efficiency and pressure ratio, but it has a lower influence on the power required and temperature ratio. The trailing edge angles, A81 and A82, corresponding to splitter 1 and splitter 2 (shorter), respectively, were more influential in the required power and temperature ratio and lower influential in isentropic efficiency. The leading edge angle, A3, corresponding to splitter 2, showed low impact on all output variables, however, its cumulative effect was close to other input parameters. The physical mechanisms are discussed in the next sections.

The definition of a cutting methodology for the input variables under study may present one or more non-influential parameters, however, the Morris histograms for the main effects indicate that the minors elementary effects have very close and impacting values on the performance of the centrifugal compressor. Figure 19 shows that input variables on output parameters have a linear behavior since they are below the reference line 2SEMi, which means that their main effects are much greater than their interaction effects. In other words, interaction effects can be considered negligible. In addition, it is evident in the graphs in Figure 19 the distance between the representative points of the input parameters in relation to the origin, emphasizing the importance of not eliminating any variable.

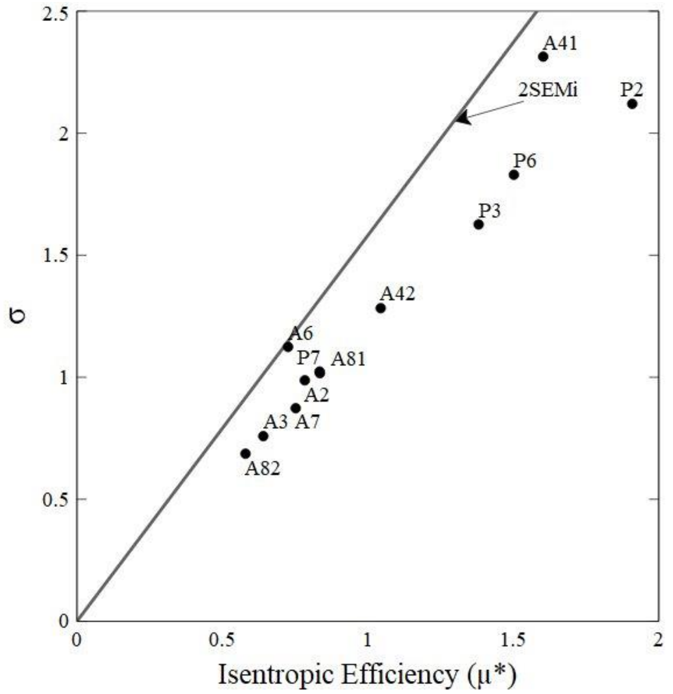

(a)

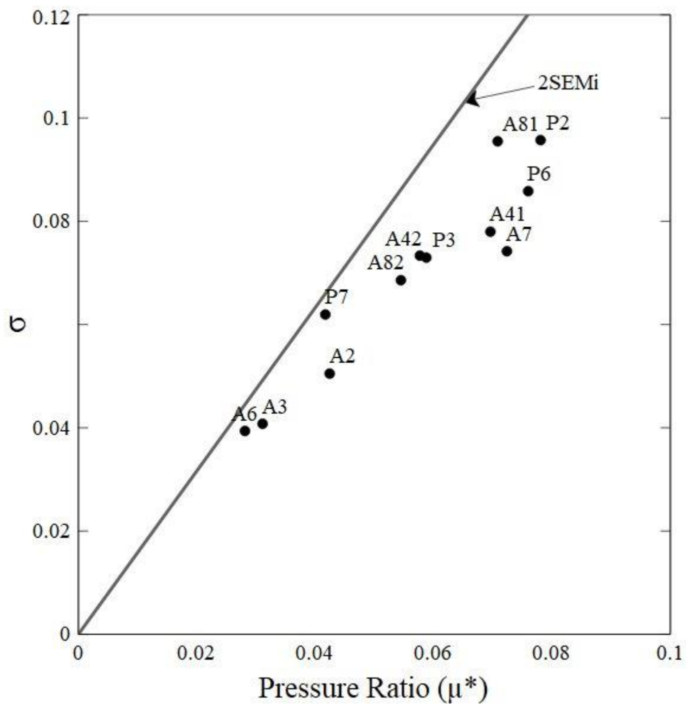

(b)

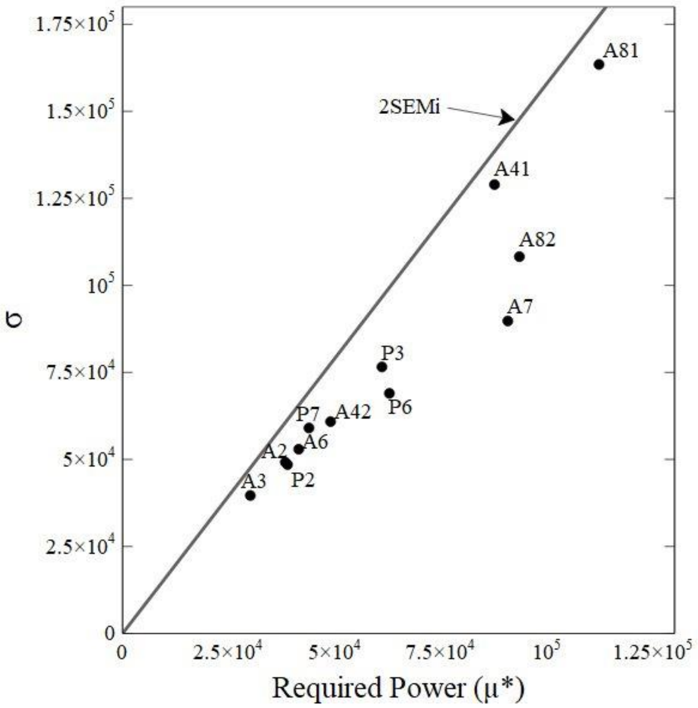

(c)

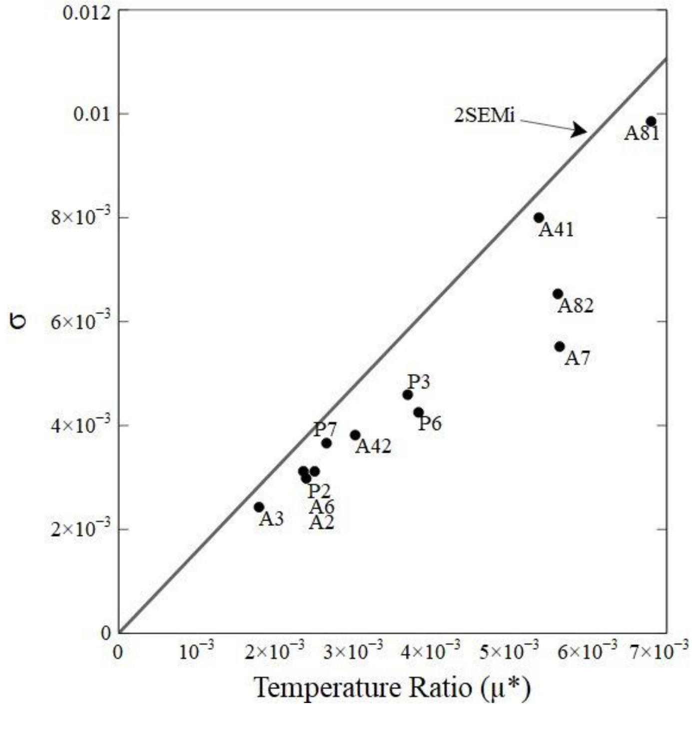

(d)

Figure 19 - Interaction effects analysis of Morris' screening method; (a) isentropic efficiency, (b) pressure ratio, (c) required power and (d) temperature ratio (Author,2024).

The effects of the geometric changes of the hub and shroud on the output parameters are shown in Figure 20 and the effects of the leading edge and trailing edge are plotted in Figure 21. The percentages are related to the impact of the variables on the absolute mean (μ*). Shroud had the most impact on isentropic efficiency in both splitters, with the leading edge position and trailing edge angles being the most influential parameters, as shown in Figures 20-a and 21-a. For the pressure ratio, the effects of changes in the hub and shroud were similar in Splitter 1 and the hub angles were more influential in Splitter 2, as shown in Figures 20-b and 21-b. For the power required and pressure ratio, the hub parameters were most influential, with emphasis on the trailing edge angles shown in Figures 20c-d and 21c-d. It should be noted that the decrease in skin friction due to smaller splitter 2 surfaces also has a minor contribution to efficiency, however, in the other output parameters the impact is similar or greater than that of splitter 1. Therefore, the performance of the centrifugal compressor can be changed significantly by combining the effects of all input variables.

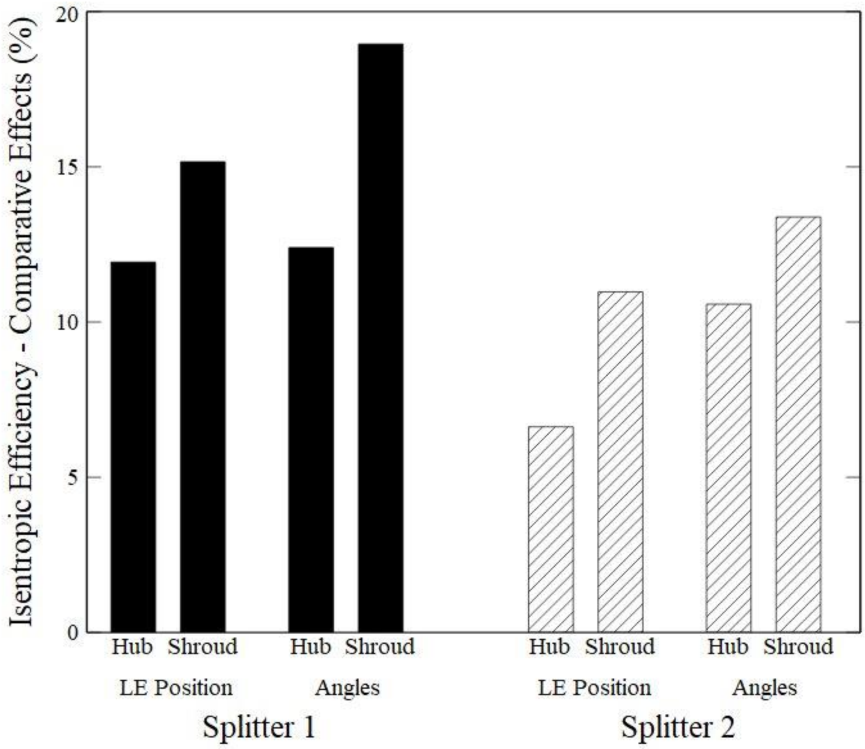

(a)

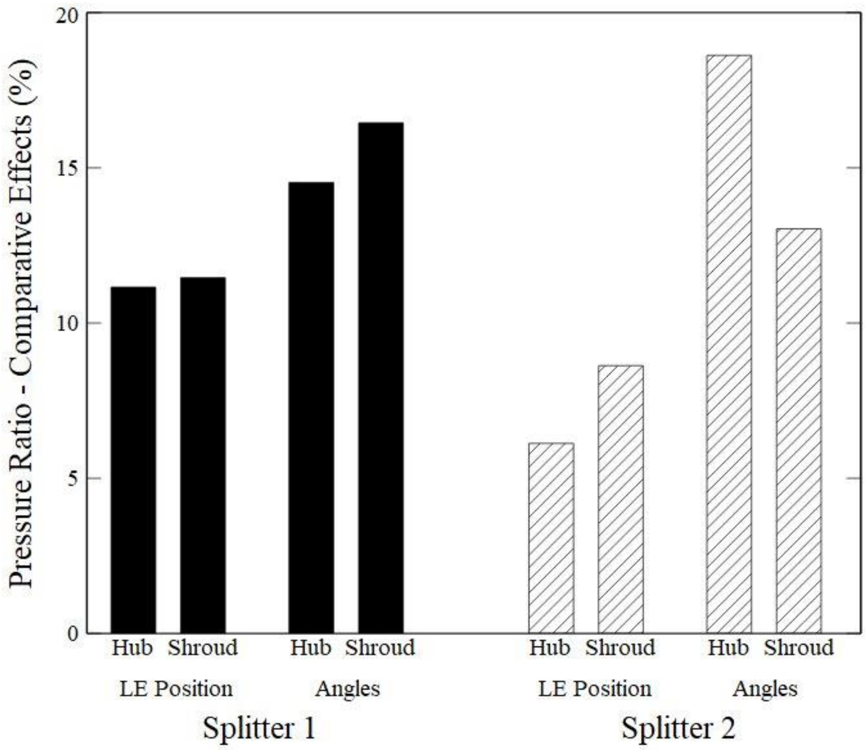
Pressure Ratio - Comparative Effects (%)
20
15
10
5
0
Hub
Shroud
Hub
Shroud
Hub
Shroud
Hub
Shroud
LE Position
Angles
LE Position
Angles
Splitter 1
Splitter 2

(b)

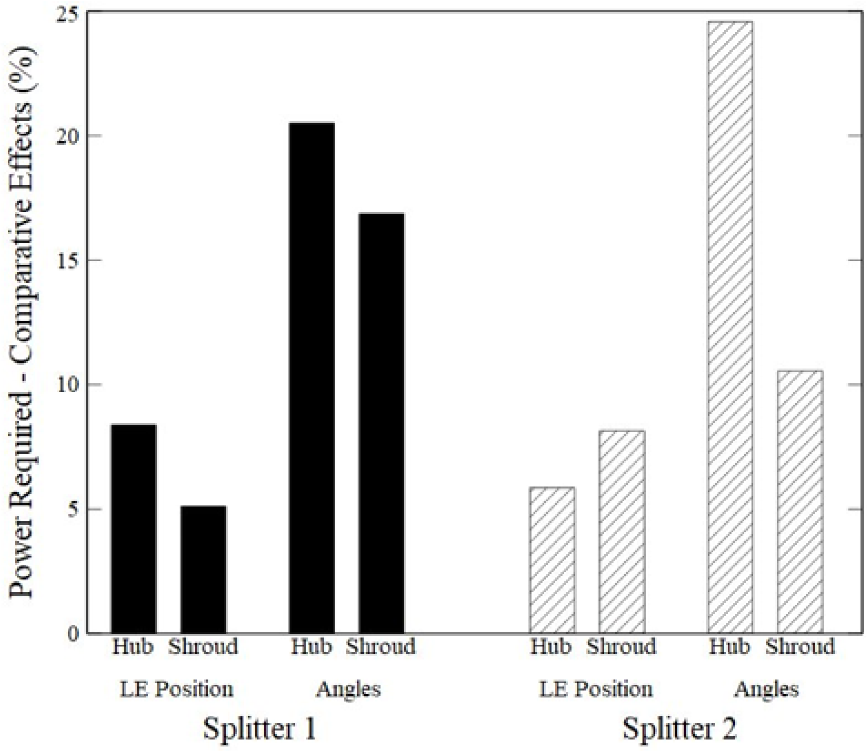
Power Required - Comparative Effects (%)
25
20
15
10
5
0
Hub
Shroud
Hub
Shroud
Hub
Shroud
Hub
Shroud
LE Position
Angles
LE Position
Angles
Splitter 1
Splitter 2

(c)

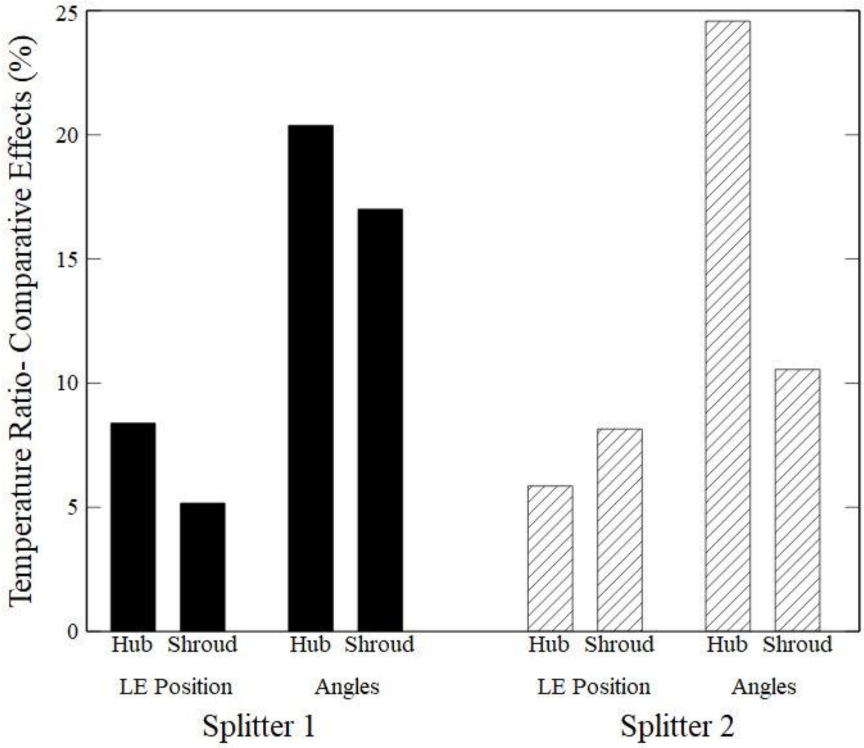

(d)

Figure 20 - Comparative effects on hub and shroud; (a) isentropic efficiency, (b) pressure ratio, (c) required power and (d) temperature ratio (Author,2024).

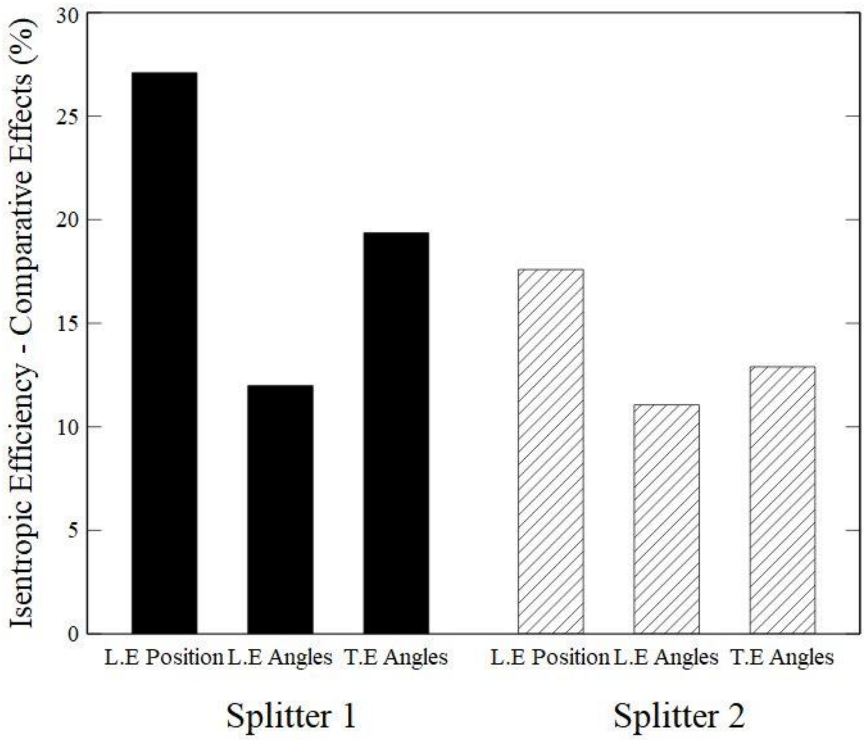

(a)

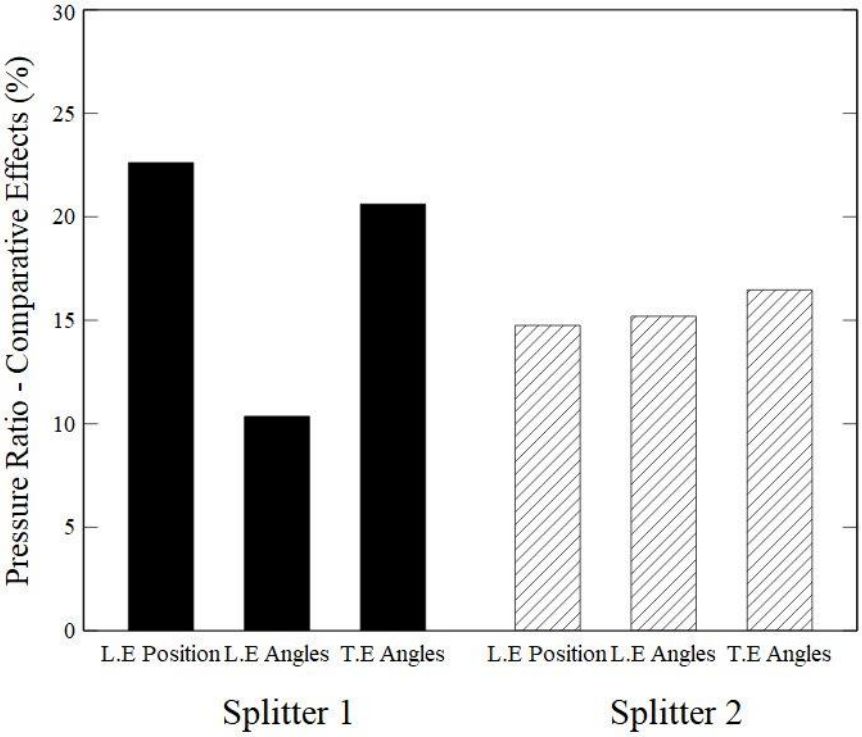
Pressure Ratio - Comparative Effects (%)
30
25
20
15
10
5
0
L.E Position
L.E Angles
T.E Angles
L.E Position
L.E Angles
T.E Angles
Splitter 1
Splitter 2

(b)

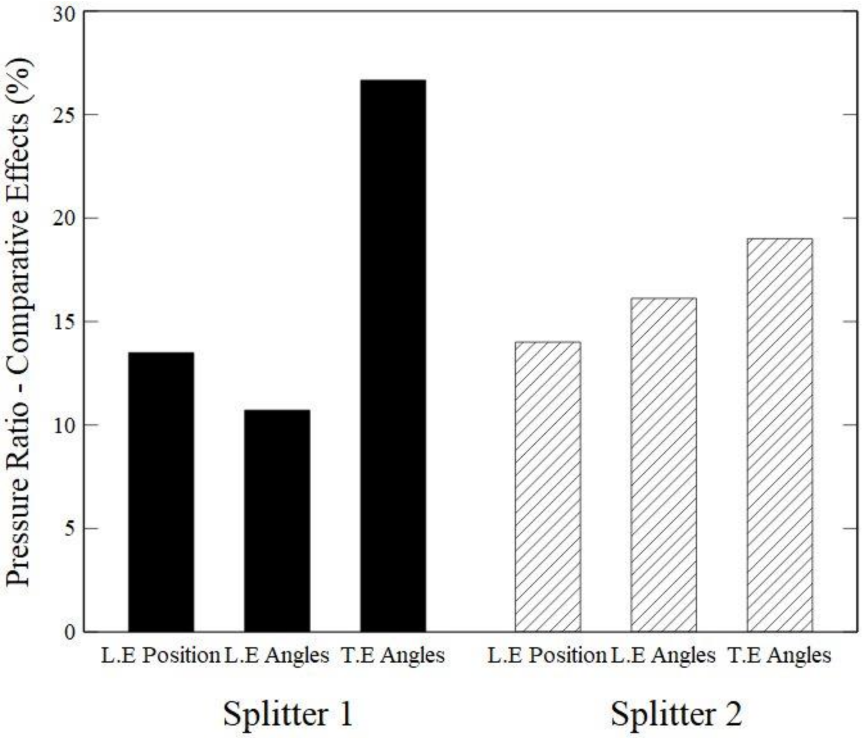
Pressure Ratio - Comparative Effects (%)
30
25
20
15
10
5
0
L.E Position
L.E Angles
T.E Angles
L.E Position
L.E Angles
T.E Angles
Splitter 1
Splitter 2

(c)

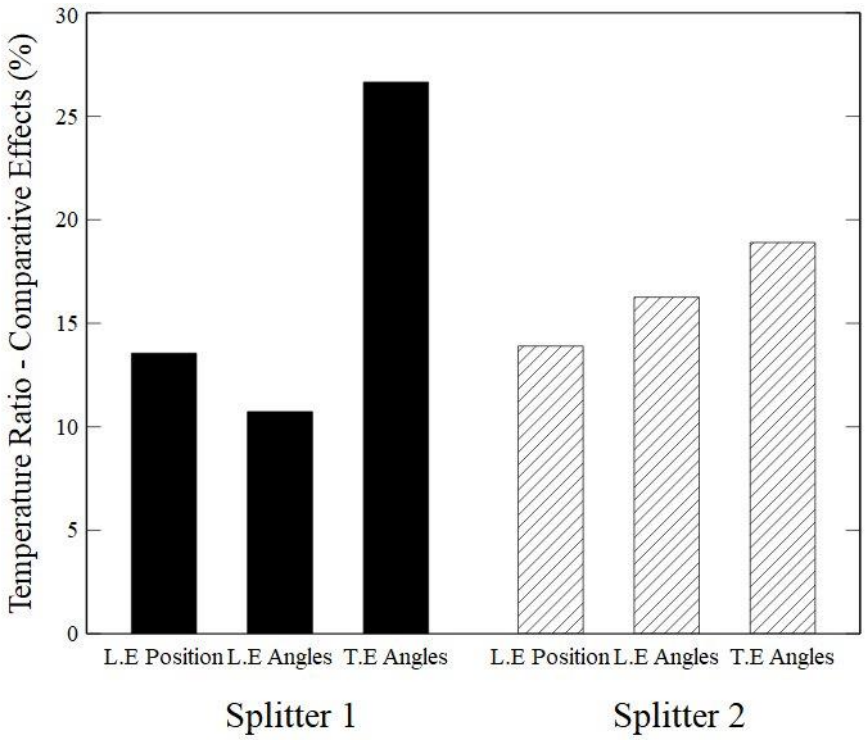

(d)

Figure 21 - Comparative effects on leading edge and trailing edge; (a) isentropic efficiency, (b) pressure ratio, (c) required power and (d) temperature ratio (Author,2024).

3.3. Phenomenology Analysis

To assess the influence of shock waves on the performance of the centrifugal compressor, two cases were studied, changing the parameter P2 by 13 mm and A2 by 1 degree, corresponding to the leading edge position and angle in splitter 1, respectively. Table 8 contains the geometric specifications of the two cases analyzed and Table 9 shows the results of the output parameters. The percentage number of elements with a Mach number greater than 1 was computed and shown in Figure 22 and contours of relative Mach number are plotted in Figure 23.

Table 8 - Input parameters.

	Leading Edge (mm)				**Angles (Degrees)**							
Variable	**P2**	**P3**	**P6**	**P7**	**A2**	**A3**	**A41**	**A42**	**A6**	**A7**	**A81**	**A82**
Model 1	30.0	108.3	50	108.3	-1	3	37.3	19.0	-0.3	0.0	42.7	29.0
Model 2	43.0	108.3	50	108.3	0	3	37.3	19.0	-0.3	0.0	42.7	29.0

Source: Author, (2024).

Table 9 - Results of leading edge changes.

	Isentropic Eff. (%)	Pressure Ratio	Temperature Ratio	Power (MW)
Model 1	81.23	3.06	1.32	5.13
Model 2	81.88	3.07	1.33	5.12
Difference	0.65%	0.33%	0.76%	0.20%

Source: Author, (2024).

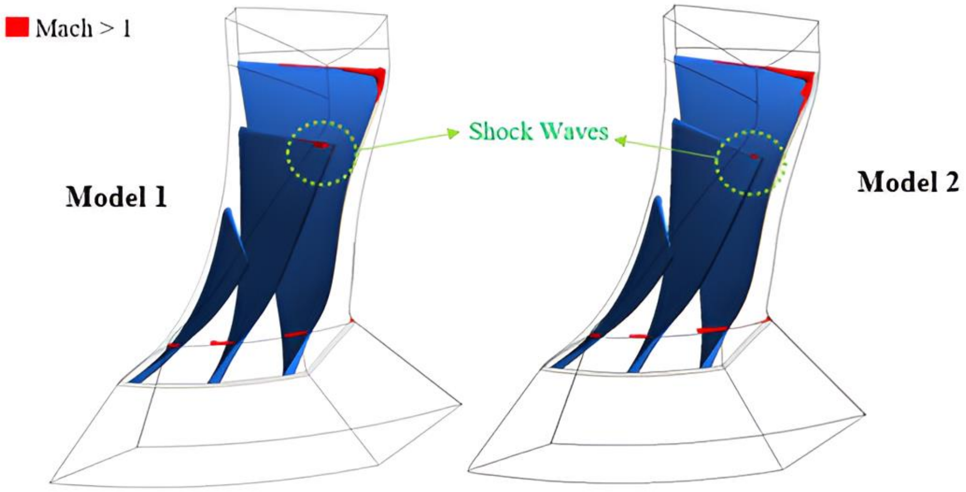

Figure 22 - Elements with relative Mach number greater than one (Author,2024).

Shock waves were identified at the leading edge of the blade and splitter 1, and in some elements at the impeller diffuser interface. The change in parameters P2 and A2 decreased the number of elements with Mach number over 1 from 3.1% to 2.2% (Figure 22), but has not totally blocked the passage, as can be seen in Figure 23. The analysis of the relative mach number close to the shroud showed an important flow blockage caused by the reverse flow near the clearance gap at the trailing edge, as reported by Michelassi [16] . There was a change in the performance of the centrifugal compressor, with a 0.65% increase in isentropic efficiency.

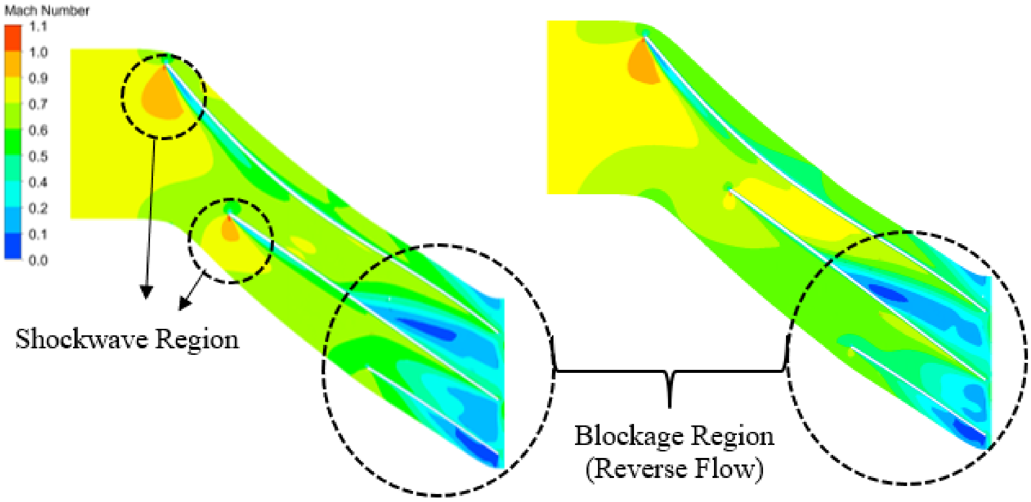

Figure 23 - Spanwise view of Mach number contours: 90% span section (Author,2024).

To quantify the influence of trailing edge angles on the overall performance of the centrifugal compressor, parameters A81 and A82 of Model 1 presented in Table 8 were varied by 1.5 degrees. These parameters are positioned, respectively, on the hub of splitters. The results obtained are presented in Table 10 and contours of relative Mach number are shown in Figure 24. The angles of the shroud were assessed separately and the physical phenomena are similar to those plotted in Figure 24.

The results presented in Table 10 show that the trailing edge angles on hub caused important impacts on outputs, especially in the pressure ratio , power required and temperature ratio, with a difference between 1.51% and 2.94%. Analysis of the blockage flow region in Figure 24 reveals changes in reverse flow, which influences the performance of the centrifugal compressor.The reverse flow found at the clearance gap is a significant source of loss, which can be verified by analysis of the static entropy chart shown in Figure 25 and blade to blade view in Figure 26. The first half of the domain is responsible for 30.8% of the increase in static entropy in the impeller due to the shock wave region. The other region containing the impeller / diffuser interface (streamwise 0.5 to 1), 69.2% of the static entropy is increased due to flow blocking.

Table 10 - Trailing edge angles analysis.

		Isentropic Eff. (%)	Pressure Ratio	Temperature Ratio	Power (MW)
Model 1	**A81= 42.7º** **A82= 29.0º**	81.23	3.06	1.32	5.13
Model 2	**A81= 44.2º** **A82= 27.5º**	81.78	3.15	1.34	5.22
Difference		0.55 %	2.94 %	1.51 %	1.75 %

Source: Author, (2024).

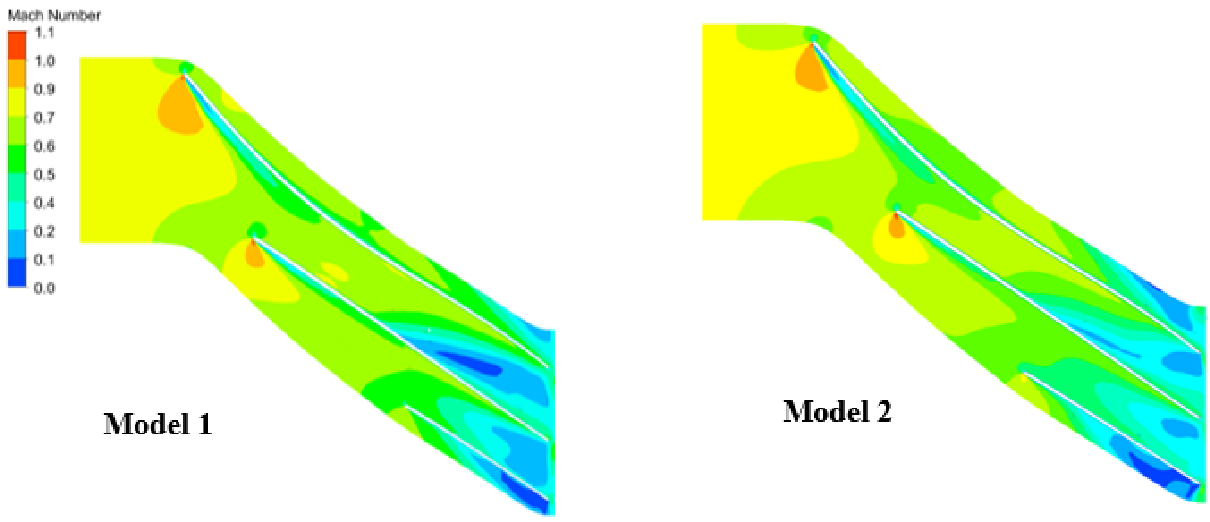

Figure 24 – Trailing edge analysis of Mach number contours: 90% span section (Author,2024).

The phenomenological analysis identified shock waves at the leading edge of the blade and splitter 1 in addition to an important blockage flow region close to the trailing edge. The geometric changes in the leading edge parameters of the splitters contribute to minimize the effects of shock waves and modify fluid flow dynamics in the reverse flow region. The trailing edge parameters that are located in the impeller / diffuser interface, in which blockage flow is noted, significantly contribute to the performance of the centrifugal compressor in the four output variables analyzed. This investigation demonstrates the importance of all the input variables studied in the operating conditions of the centrifugal compressor.This physical phenomenon assessment is in agreement with SA predictions, reinforcing that the Morris' screening method is a robust and reliable methodology for turbomachinery CFD models analysis.

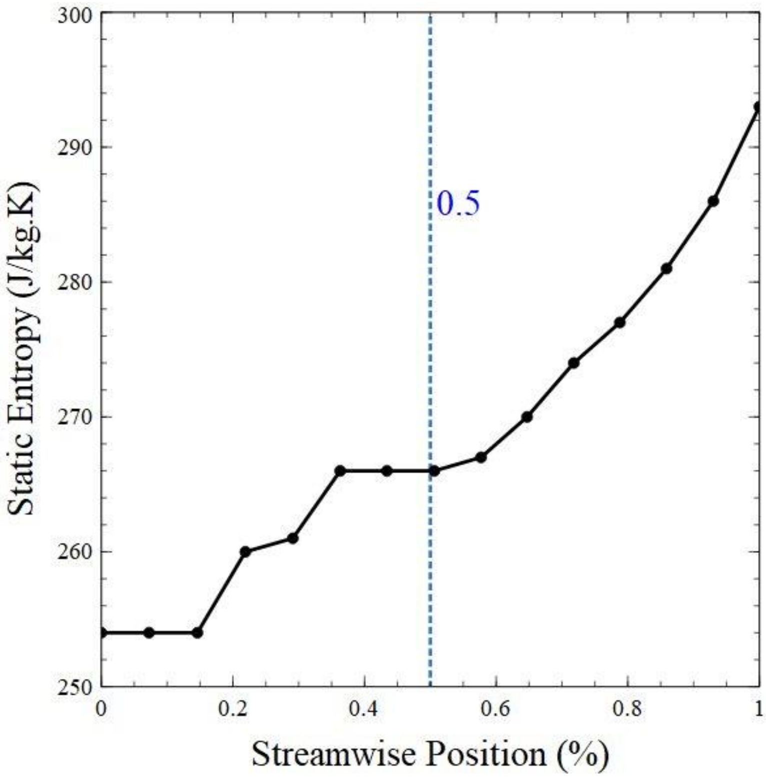

Figure 25 - Impeller static entropy chart in spanwise view (Author,2024).

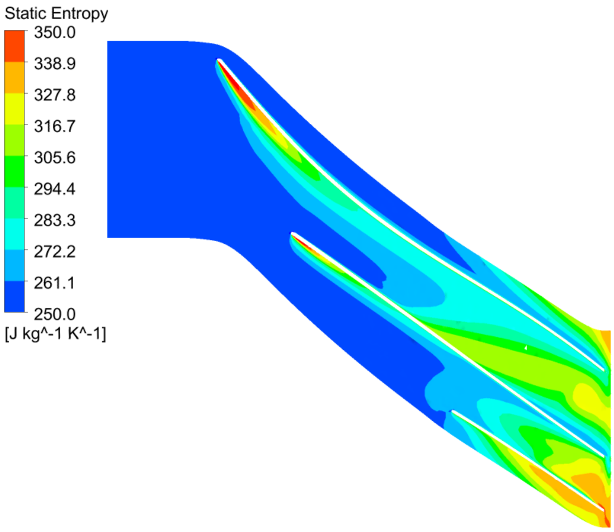

Figure 26 – Impeller static entropy: 90% span section (Author,2024).

4. CONCLUSION

In this research, the position of the leading edge and the camber angles of two splitters added to the impeller are the geometric parameters evaluated in the numerical simulation and submitted to a sensitivity analysis methodology in order to identify their influence on the performance of the centrifugal compressor.The CO_2 centrifugal compressor is modeled as a periodical tridimensional domain, steady-state and turbulent. In total, 12 input parameters were parameterized, 4 related to the position of the leading edge and 8 to the camber angles. The major findings are summarized as follows:

- The insertion of two splitters in the impeller changed the performance of the centrifugal compressor. In the 130 CFD cases analyzed, a range of 4.4% in isentropic efficiency and 8.1% in pressure ratio was observed.
- The sensitivity analysis by the Morris' method identified a significant impact of all the input parameters studied on the output variables. The longer splitter located close the suction surface was influential in all output variables, especially the position of the leading edge and the angles of the trailing edge. The shorter splitter close to the pressure surface was highlighted by the hub angles, which significantly impacted the pressure ratio, required power and temperature ratio.
- The phenomenological analysis of the dynamic flow found a significant source of losses at the leading-edge due to shockwave and at the trailing-edge due to the flow blockage, with the reverse flow responsible for most of the addition of static entropy in the impeller.
- The usage of Morris' method in turbomachinery is a promising tool that can increase effectively the number of parameters of a design allowing the simultaneous study of their impact on the equipment performance.

5. BIBLIOGRAPHY

[1] M. P.Boyce, *Centrifugal Compressors: A Basic Guide*, 1st ed. Tulsa,Oklahoma, 2003.

[2] T. NORTON and D. W. SUN, “Computational fluid dynamics (CFD) - an effective and efficient design and analysis tool for the food industry: A review,” *Trends Food Sci. Technol.*, vol. 17, no. 11, pp. 600–620, 2006.

[3] C. P. da F. L. Raynal, F. Augier, F. Bazer-Bachi, Y. Haroun, “CFD Applied to Process Development in the Oil and Gas Industry - A Review,” *Oil Gas Sci. Technol.*, vol. 71, no. 3, 2016.

[4] S. Kim, “The effects of foreign direct investment, economic growth, industrial structure, renewable and nuclear energy, and urbanization on Korean greenhouse gas emissions,” *Sustain.*, vol. 12, no. 4, 2020, doi: 10.3390/su12041625.

[5] W. P. Limited, *Developments and innovation in carbon dioxide (CO2) capture and storage technology*. Limited, Woodhead Publishing, 2010.

[6] K. H. Lüdtke, *Process Centrifugal Compressors: Basics, Function, Operation, Design, Application*. Berlin: Springer, 2004.

[7] S. S. SANGHERA, “Centrifugal Compressor Meanline Design Using Real Gas Properties,” no. April, p. 29, 2013.

[8] H. I. H. Saravanamuttoo *et al.*, *Gas Turbine Theory*, 7th ed. New York: Pearson, 2017.

[9] M. Heinrich, “Genetic Optimization of Turbomachinery Components using the Volute of a Transonic Centrifugal Compressor as a Case Study.” p. 117, 2016.

[10] C. Xu and R. S. Amano, “Centrifugal Compressor Performance Improvements Through Impeller Splitter Location,” *J. Energy Resour. Technol. Trans. ASME*, 2018, doi: 10.1115/1.4037813.

[11] A. Hehn, M. Mosdzien, D. Grates, and P. Jeschke, “Aerodynamic optimization of a transonic centrifugal compressor by using arbitrary blade surfaces,” *J. Turbomach.*, 2018, doi: 10.1115/1.4038908.

[12] S. A. Moussavi, A. Hajilouy Benisi, and M. Durali, “Effect of splitter leading edge location on performance of an automotive turbocharger compressor,” *Energy*, vol. 123, pp. 511–520, 2017, doi: 10.1016/j.energy.2017.02.011.

[13] E. L. J. Bohez, S. D. R. Senadhera, K. Pole, J. R. Duflou, and T. Tar, “A Geometric Modeling and Five-Axis Machining Algorithm for Centrifugal Impellers,” *J. Manuf. Syst.*, vol. 16, no. 6, pp. 422–436, 1997, doi: 10.1016/S0278-6125(97)81700-1.

[14] M. Oana, O. Kawamoto, H. Ohtani, and Y. Yamamoto, “Approach to High-Performance Transonic Compressor Design,” *J. Propuls. Power*, vol. 20, no. 1, pp. 164–170, 2004, doi: 10.2514/1.9243.

[15] A. Lohmberg, M. Casey, and S. Ammann, “Transonic radial compressor inlet design,” *Proc. Inst. Mech. Eng. Part A J. Power Energy*, vol. 217, no. 4, pp. 367–374, 2003, doi: 10.1243/095765003322315423.

[16] R. R. Erdmenger and V. Michelassi, “Impact of Main and Splitter Blade Leading Edge Contour on the Performance of High Pressure Ratio Centrifugal Compressors,” *ASME Turbo Expo 2014*, pp. 1–13, 2014.

[17] M. W. Layth H, Jawad S, Abdullah, Zulkifli R, “Numerical simulation of flow inside a modified turbocharger centrifugal compressor,” *Asian J. Appl. Scienses*, vol. 5, pp. 53–72, 2012.

[18] A. Malik, Q. Zheng, A. A. Zaidi, and H. Fawzy, “Performance enhancement of centrifugal compressor with addition of splitter blade close to pressure surface,” *J. Appl. Fluid Mech.*, vol. 11, no. 4, pp. 919–928, 2018, doi: 10.18869/acadpub.jafm.73.247.28658.

[19] M. CASEY and C. ROBINSON, “A Method to Estimate the Performance Map of a Centrifugal Compressor Stage,” *J. Turbomach.*, vol. 135, no. 2, p. 021034, 2012.

[20] P. Dalbert, B. Ribi, T. Kmeci, and M. V. Casey, “Radial compressor design for industrial compressors,” *Proc. Inst. Mech. Eng. Part C J. Mech. Eng.*, vol. 213, no. 1, pp. 71–83, 1999, doi: 10.1243/0954406991522194.

[21] C. Rodgers, “THE CENTRIFUGAL COMPRESSOR INDUCER,” *Cranf. Univ. Short Course Centrif. Compressors*, vol. 5, p. 5, 1998.

[22] E. Benini, A. Toffolo, and A. Lazzaretto, “Experimental and numerical analyses to enhance the performance of a microturbine diffuser,” *Exp. Therm. Fluid Sci.*, 2006, doi: 10.1016/j.expthermflusci.2005.09.003.

[23] R. H. Aungier, “A fast, accurate real gas equation of state for fluid dynamic analysis applications,” *J. Fluids Eng. Trans. ASME*, 1995, doi: 10.1115/1.2817141.

[24] P. R. Spalart and M. Shur, “On the Sensitization of Turbulence Models to Rotation and Curvature,” *Aerosp. Sci. Technol.*, vol. 1, no. 5, pp. 297–302, 1997, doi: 10.1016/S1270-9638(97)90051-1.

[25] I. B. U. G. Celik, P. J. Roache, and C. J. F. H. C. P. E. Raad, “Procedure for Estimation and Reporting of Uncertainty Due to Discretization in CFD Applications,” *J. Fluids Eng.*, vol. 130, no. 7, p. 078001, 2008, doi: 10.1115/1.2960953.

[26] M. D. Morris, “Factorial Sampling Plans for Preliminary Computational Experiments,” *Technometrics*, vol. 33, pp. 161–174, 1991, doi: 10.1177/001872086700900503.

[27] A. SALTELLI, M. RATTO, T. ANDRES, F. CAMPOLONGO, J. CARIBONI, and D. GATELLI, “Global Sensitivity Analysis. The Primer.” John Wiley & Sons Ltd, West Sussex, England, 2008.

[28] F. CAMPOLONGO, J. CARIBONI, and A. SALTELLI, “From screening to quantitative sensitivity analysis. A unified approach,” *Comput. Phys. Commun.*, vol. 182, no. 4, pp. 978–988, 2011.

[29] F. Campolongo, J. Cariboni, and A. Saltelli, “An effective screening design for sensitivity analysis of large models,” *Environ. Model. Softw.*, vol. 22, no. 10, pp. 1509–1518, 2007, doi: 10.1016/j.envsoft.2006.10.004.

[30] F. CAMPOLONGO, J. CARIBONI, and A. SALTELLI, “An effective screening design for sensitivity analysis of large models,” *Environ. Model. Softw.*, vol. 22, no. 10, pp. 1509–1518, 2007.

[31] P. A. Vanrolleghem, G. Mannina, A. Cosenza, and M. B. Neumann, “Global sensitivity analysis for urban water quality modelling: Terminology, convergence and comparison of different methods,” *J. Hydrol.*, vol. 522, pp. 339–352, 2015, doi: 10.1016/j.jhydrol.2014.12.056.

[32] M. Casey and C. Robinson, “A new streamline curvature throughflow method for radial turbomachinery,” 2008, doi: 10.1115/GT2008-50187.

[33] ANSYS, *CFX - Solver Theory Guide*. Canonsburg, U.S.: ANSYS, Inc., 2006.

[34] F. R. Menter, “Review of the shear-stress transport turbulence model experience from an industrial perspective,” *Int. J. Comut. Fluid Dyn.*, vol. 23, no. 4, pp. 305–316, 2009, doi: 10.1080/10618560902773387.

[35] T. Knopp, T. Alrutz, and D. Schwamborn, “A grid and flow adaptive wall-function method for RANS turbulence modelling,” *J. Comput. Phys.*, vol. 220, no. 1, pp. 19–40, 2006, doi: 10.1016/j.jcp.2006.05.003.